



12-2005

# A Study of Material Properties and Relevant Microstructure Parameters that May Influence the $V_{50}$ Ballistic Limit Velocity of Composite Ceramics

Adolphus McDonald  
*University of Tennessee, Knoxville*

---

## Recommended Citation

McDonald, Adolphus, "A Study of Material Properties and Relevant Microstructure Parameters that May Influence the  $V_{50}$  Ballistic Limit Velocity of Composite Ceramics. " Master's Thesis, University of Tennessee, 2005.  
[https://trace.tennessee.edu/utk\\_gradthes/4589](https://trace.tennessee.edu/utk_gradthes/4589)

This Thesis is brought to you for free and open access by the Graduate School at Trace: Tennessee Research and Creative Exchange. It has been accepted for inclusion in Masters Theses by an authorized administrator of Trace: Tennessee Research and Creative Exchange. For more information, please contact [trace@utk.edu](mailto:trace@utk.edu).

To the Graduate Council:

I am submitting herewith a thesis written by Adolphus McDonald entitled "A Study of Material Properties and Relevant Microstructure Parameters that May Influence the  $V_{50}$  Ballistic Limit Velocity of Composite Ceramics." I have examined the final electronic copy of this thesis for form and content and recommend that it be accepted in partial fulfillment of the requirements for the degree of Master of Science, with a major in Engineering Science.

Roy J. Schulz, Major Professor

We have read this thesis and recommend its acceptance:

Basil N. Antar, Ahmad D. Vakili

Accepted for the Council:

Carolyn R. Hodges

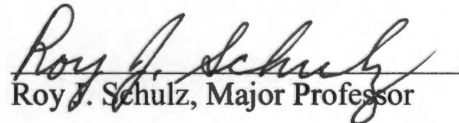
Vice Provost and Dean of the Graduate School

(Original signatures are on file with official student records.)

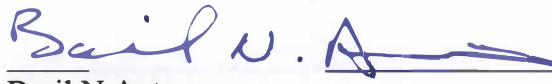
---

To the Graduate Council:

I am submitting herewith a thesis written by Adolphus McDonald entitled "A Study of Material Properties and Relevant Microstructure Parameters that May Influence the  $V_{50}$  Ballistic Limit Velocity of Composite Ceramics". I have examined the final paper copy of this thesis for form and content and recommend that it be accepted in partial fulfillment of the requirements for the degree of Master of Science, with a major in Engineering Science.

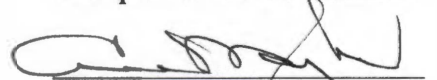
  
Roy J. Schulz, Major Professor

We have read this thesis and  
recommend its acceptance:

  
Basil N. Antar

  
Ahmad D. Vakili

Acceptance for the Council:

  
Vice Chancellor and Dean of  
Graduate Studies

THE UNIVERSITY OF CHICAGO  
DIVISION OF THE PHYSICAL SCIENCES  
DEPARTMENT OF CHEMISTRY  
505 EAST HALL  
CHICAGO, ILLINOIS 60607-7055  
TEL: 773-936-5200 FAX: 773-936-5201  
WWW.CHEM.UCHICAGO.EDU

Thesis  
2005  
.m226

Thesis  
2005  
.m226

THE UNIVERSITY OF CHICAGO  
DIVISION OF THE PHYSICAL SCIENCES  
DEPARTMENT OF CHEMISTRY  
505 EAST HALL  
CHICAGO, ILLINOIS 60607-7055  
TEL: 773-936-5200 FAX: 773-936-5201  
WWW.CHEM.UCHICAGO.EDU

Thesis  
2005  
.m226

Thesis  
2005  
.m226

UNIVERSITY OF CHICAGO  
DIVISION OF THE PHYSICAL SCIENCES  
DEPARTMENT OF CHEMISTRY  
505 EAST HALL  
CHICAGO, ILLINOIS 60607-7055  
TEL: 773-936-5200 FAX: 773-936-5201  
WWW.CHEM.UCHICAGO.EDU

Thesis  
2005  
.m226

**A STUDY OF MATERIAL PROPERTIES  
AND  
RELEVANT MICROSTRUCTURE PARAMETERS  
THAT  
MAY INFLUENCE THE  $V_{50}$  BALLISTIC LIMIT VELOCITY OF COMPOSITE  
CERAMICS**

**A Thesis  
Presented for the  
Master of Science  
Degree  
The University of Tennessee, Knoxville**

**Adolphus McDonald  
December, 2005**

**Copyright © 2005 by Adolphus McDonald, Jr.  
All rights reserved.**

## **DEDICATION**

This thesis is dedicated to my father; Adolphus McDonald, Sr. who recently died of cancer. He was a role model, loving father, friend, and mentor. In addition, the thesis is dedicated to my mother Emma Jean McDonald and the rest of the family as well, for always believing in me, and inspiring me to excel in whatever endeavor or goals I set for myself.





## **Acknowledgment**

I wish to thank all those who helped me complete my Master of Science degree in Engineering Science. I express my gratitude to my former advisor for the first three year at University Tennessee Space Institute, Dr. Mary Helen McCay for giving me the opportunity to start the Masters Program in her group. I would like to specially thank to my current advisor, Dr. Roy J. Schulz, for all his help and guidance. I would like to thank Russell Prather of the U.S. Army Research Laboratory for the use of his ballistic test facility. I would like to thank the A. Boigenzahn, M. Kragness, and Rosalind Batson of Clear Science, and Al Ingram and Scott Patterson of the U.S. Army Aviation and Missile Research, Development, and Engineering Center, for assisting me in the material preparation and analysis. I would like to give special thanks to Tanya Litvinas of the U.S. Army Research, Development, and Engineering Command, Comparative Testing Office for providing the funds to support the testing and evaluation of ballistic armor technology from foreign companies.



## **Abstract**

The purpose of this research is to evaluate, compare, and correlate the microstructure and mechanical properties of a selected group of ceramic armor samples to the  $V_{50}$  ballistic limit velocity. This study is to identify any relation between the desired material properties and the relevant microstructure parameters that significantly influence the ballistic limit velocity. The ceramic materials, silicon carbide and boron carbide, were produced and provided by five foreign companies. These companies were under contract by the United States Army, Research, Development, and Engineering Command to provide ceramic armor for comparative testing and material evaluation.

Ballistic testing was carried out to determine the  $V_{50}$  ballistic limit velocity for each ceramic material; mechanical testing of each ceramic material was performed to obtain material density, microindentation hardness, and flexural strength. Ceramography analysis of the material was also carried out to characterize the microstructure for each material.

Results showed that the ranges in these properties of the ceramic materials properties were determined as follows: Flexural strength ranged from 385 to 683 MPa, Knoop hardness ranged from 2,200 to 3258  $\text{kgf/mm}^2$ , density ranged from 3.1659 to 3.2376  $\text{g/cm}^3$ , grain size ranged from 5 to 15  $\mu\text{m}$ , and porosity ranged from 2 to 10%. The ballistic limit velocities for these ceramic materials ranged from 292 to 372 m/s.

The ballistic limit velocity was well correlate with the ceramic flexural strength. Other material property such as density, microindentation hardness, and grain size did not directly correlate with the ballistic performance. The porosity of these ceramic

materials did somewhat correlated with ballistic performance data dispersion or scatter, with increased scatter occurring at higher porosity levels.

As a note, the ballistic tests were done on the composite laminated ceramic but the material and microstructure properties in this study only refer to the ceramic materials. The front and backing fibrous material that comprised of the composite laminated ceramic was not considered in the material analysis of this study. It is my estimation and experience from testing and evaluating ballistic armor that the ceramic provides approximately 90% to 95% in the erosion process and breaking up the steel core projectile. The fibrous material accounts for approximately 5% to 10% in stopping residual fragments and absorbing the kinetic energy. Therefore, the main focus was on the ceramic properties influence on  $V_{50}$  ballistic limit.

## Table of Contents

Chapter 1 .....	1
Introduction.....	1
Chapter 2 .....	3
Review of Literature .....	3
Chapter 3 .....	7
Methodology .....	7
3.1    Experimental Setup for Ballistic Testing of Ceramic Armor Samples.....	7
3.2    Sample Preparation for Characterization of Sample Physical Properties..	10
Chapter 4 .....	15
Results and Discussions.....	15
4.1    Optical Micrographs .....	15
4.2    Scanning Electron Microscopy .....	16
4.3    X-Ray Diffraction .....	17
4.4    Flexural Tests.....	18
4.5    Microindentation Measurements .....	19
4.6    Density Measurements .....	20
4.7    Material Comparison .....	21
4.8    Ballistic Testing .....	22
4.9    Material and Microstructure Properties vs. $V_{50}$ Ballistic Limit.....	23
Chapter 5 .....	27
Conclusion .....	27
Chapter 6 .....	29
Recommendations.....	29
List of Reference.....	31
Appendices.....	35
Appendix A.....	37
Appendix B.....	53

Appendix C.....	59
Ceramography Protocols .....	60
X-Ray Diffraction Test Protocol .....	61
Flexure Testing Protocol .....	61
Microindentation Measurement Protocol .....	62
Density Measurements Protocol.....	62
Appendix D .....	63
X-Ray Diffraction (XRD) Plots.....	64
Vita .....	69

## **List of Tables**

Table B-1: Summary of Ceramic Composite Ballistic Materials .....	54
Table B-2: Summary of Projectile Physical Dimension .....	54
Table B-3: Summary of 3-Point Bending Flexural Strength (MPa) .....	54
Table B-4: Summary of Microindentation Hardness Measurements ( $\text{kgf/mm}^2$ ) .....	55
Table B-5: Summary of Density Measurements ( $\text{g/cm}^3$ ) .....	55
Table B-6: Ceradyne's Silicon Carbide and Boron Carbide Ceramic Property .....	56
Table B-7: Single Shots Ballistic Results of the Ceramic Opaque Composite Armors	57
Table C-1: Polishing Procedure for Silicon Carbide and Boron Carbide .....	60





## List of Figures

Figure A-1: Laminate Armor Options .....	38
Figure A-2: Penetrator Defeat Mechanism .....	38
Figure A-3: Illustration of Ballistic Test Setup.....	39
Figure A-4: Steel Frame Mounting Bracket.....	39
Figure A-5: 12.7 x 108 mm Armor Piercing Incendiary .....	40
Figure A-6: Etched Microstructures of Ceramic Materials Analyzed .....	41
Figure A-7: Unetched Microstructures of Ceramic Materials Analyzed.....	42
Figure A-8: Grain Size and Porosity of Samples.....	43
Figure A-9: Scanning Electron Microscopy of Materials Analyzed at 500x.....	44
Figure A-10: Scanning Electron Microscopy of Materials Analyzed at 2500x.....	45
Figure A-11: Flexural Strength (at brittle fracture) from 3-Point Bending of Samples	46
Figure A-12: Statistical Analysis of Samples Flexural Strength .....	46
Figure A-13: Microindentation Hardness of Samples .....	47
Figure A-14: Statistical Analysis of Samples Microindentation Hardness .....	47
Figure A-15: Density Measurement of Samples.....	48
Figure A-16: Statistical Analysis of Samples Density .....	48
Figure A-17: Single Shot Ballistic Results of Ceramic Samples.....	49
Figure A-18: $V_{50}$ Ballistic Limit Velocity and Flexural Strength.....	49
Figure A-19: $V_{50}$ Ballistic Limit Velocity and Knoop Hardness.....	50
Figure A-20: $V_{50}$ Ballistic Limit Velocity and Density.....	50
Figure A-21: $V_{50}$ Ballistic Limit Velocity and Grain Size .....	51
Figure A-22: $V_{50}$ Ballistic Limit Velocity and Porosity .....	51



## Nomenclature

cc	cubic centimeter
g	gram
m	meter
mm	millimeter
$\mu\text{m}$	micrometer
$\text{g}/\text{cm}^3$	grams/cubic centimeter
$\text{kg}/\text{sq. m}$	kilogram/square meter
m/s	meters/second

## Abbreviations

API	Armor Piercing Incendiary
ARL	Army Research Laboratory
CVD	Chemical Vapor Deposition
$\text{CuK}\alpha$	Copper K alpha
EDS	Energy Dispersive X-Ray Spectroscopy
HK	Knoop hardness number
HP	Hot Pressing
Kevlar	Aramid Fiber
KOH	Potassium Hydroxide
PDF	Powder Diffraction File
RDECOM	Research, Development, and Engineering Command
RDE&T	Research, Development, Test and Evaluation
SEM	Scanning Electron Microscopy
Spectra	High Performance Polyethylene (HPPE)
S2	High Strength Glass Fiber
$V_{50}$	Ballistic Limit Velocity
XRD	X-Ray Diffraction



# **Chapter 1**

## **Introduction**

Over the past 45 years, research and development of ceramic materials for armor applications have been of great interest to the United States Army. A major initiative for armor research occurred in the early 1960's during the Vietnam War, when the United States Army required protection for helicopter pilots and key components of helicopters (Matchen, 1996). Forty five years later with the experience of Operation Iraqi Freedom, there is a major initiative by the U.S. Army to provide armor protection for ground vehicles, soldiers, and weapon systems for combat.

The United States Army Research, Development, and Engineering Command (RDECOM) is developing and evaluating new technologies for lightweight armor materials and their integration into current and future army aviation platforms, missiles, launchers, and vehicles. For the material developers to meet a broad range of mission requirements, future weapon systems are required to do more with less weight and size. Therefore, development and evaluation of lightweight armor material is critical for future lightweight armor package systems. The Army's concept for lightweight armor is important for maneuverability, and weapon systems must be light in order for combat units to deploy quickly.

Ceramics are well suited for application to lightweight armor because of their high physical properties and low density. The main requirement for ceramic armor is to stop small armor-piercing projectiles and high velocity fragments, and also be lighter than the equivalent metal armor. One of the first lightweight armor systems that

provided protection against ballistic projectiles was composed of a sintered aluminum oxide ceramic tile, approximately one third of an inch thick, bonded to a ductile backing panel, which was usually aluminum or fiberglass reinforced plastic (Matchen, 1996).

Figure A-1<sup>1</sup> shows several laminate armor options that are of current interest.

The two-component lightweight armor systems are very effective when struck by a high velocity projectile because the core or penetrator is broken up upon impact or eroded by the hardened face of the ceramic. Then the backing plate absorbs residual energy from ballistic impact and also serves as a “catcher’s mitt” to catch any residual fragments. The penetrator-defeat mechanisms are illustrated in Figure A-2.

---

<sup>1</sup> All figures are located in Appendix A.

## **Chapter 2**

### **Review of Literature**

A ballistic limit exists for high velocity projectiles that penetrate into materials, including ceramics, solely based on the projectile kinetic energy, and it is affected by many parameters. Among these parameters are the projectile geometry (length, diameter, and nose shape), hardness, density, yield strength, pitch and yaw angles at impact. The target parameters include thickness, hardness, density, grain and porosity characteristics, yield strength, and fracture toughness. The target microstructure features are the grain size, percent free volume or porosity, grain and porosity cell shape, surface, and homogeneity which affect the physical and ballistic properties of the material.

Within the last ten years, research and development of ceramic-based armor has significantly advanced the understanding of the effects of ceramic microstructure and mechanical properties on the ceramic ballistic performance. There has been a considerable amount of work done to correlate ceramic microstructure and mechanical properties to ceramic ballistic performance. Adams et al. (2001) focused their research on microstructure control during fabrication and the correlation of microstructure with mechanical properties and penetration resistance of ceramic composites. Lach (1993) has studied the ballistic performance of ceramics against kinetic energy projectiles; his work revealed that flexural strength seems to have a slightly greater influence on the ballistic performance than other mechanical values. Rozenberg and Yeshurun (1988) conducted experiments that demonstrated a clear relationship between ballistic

efficiency and the effective compressive strength of ceramics, where ballistic efficiency ( $\eta$ ) is the slope of the straight line through the experimental points is expressed in terms of  $h_c^*$ , the minimum tile thickness needed to prevent penetration into the backing,  $P_B^*$ , the penetration depth of the same projectile into a bare metal backing plate, and  $\rho_B$  and  $\rho_c$  which are the densities of the metal backing plate and the ceramic, respectively:

$$\eta = \frac{\rho_B P_B^*}{\rho_c h_c^*} \quad (2.1)$$

The main properties of ceramics which affect the ballistic performance were examined and analyzed by Medvedovski (2002), who concluded that it was the combination of microstructure and mechanical properties that influences ballistic performance. Work by Faber and Meyer (1995) showed from ballistic tests that the ballistic performance of a ceramic increases with increasing hardness, and the work by Krell and Blank (1995) demonstrated that the hardness of a ceramic increases with decreasing grain size which is also true of metals. Krell et al. (2002) did work that showed that hardness is much more important for ballistic performance than bending strength. Bartkowski and Spletzer (2001) examined and observed the microstructure of silicon carbide; from their work they concluded that the elastic constant (Young's Modulus) increases as the volume fraction of increased.

The primary goal of the present research study is to evaluate, compare, and correlate microstructure and mechanical properties of a selected group of ceramic armor samples to the  $V_{50}$  ballistic limit. The purpose of the study is to identify any relation between the desired material properties and the relevant microstructure parameters that significantly influence the ballistic limit. For this purpose, ballistic armor ceramic



samples were provided to the United States Army Research, Development, and Engineering Command (RDECOM) by companies from the United Kingdom of Great Britain, Canada, Germany, and Australia for ballistic testing and material analysis.

The results of the material analysis and ballistic testing were obtained by conducting a ceramography analysis to characterize each sample material by its grain size, porosity, and density. Mechanical testing was conducted to determine the flexural strength and microindentation hardness of the materials. And finally, tests of the samples under ballistic impact were also conducted. A series of plots showing both the material analysis results and the ballistic testing results were prepared and the material property of each sample was compared to that material's ballistic performance.



## **Chapter 3**

### **Methodology**

#### **3.1 Experimental Setup for Ballistic Testing of Ceramic Armor Samples**

##### **3.1.1 Experimental Setup**

The experimental ballistic tests were conducted according to the MIL-STD-666F which describes the general guidelines for procedures, equipment, physical conditions, and terminology for determining the ballistic resistance of metallic, nonmetallic and composite armor against small arms projectiles (Military Standard, 1997). The method of the standard is intended for use in ballistic acceptance testing of armor and for the research and development of new armor material. Shown in Figure A-3 is the experimental test setup which consisted of a launch weapon, breakscreens, yaw card, test samples, mounting bracket, witness panel, and projectile. The test weapon was positioned at a specified distance from the test samples which were set perpendicular to line of sight of the gun barrel. Samples were rigidly mounted to a square test frame shown in Figure A-4. Positioned behind the square test frame at a distance of 152 millimeters (mm) was a 0.5 mm thick 2024 T3 aluminum witness plate used to establish whether there was partial or complete penetration of the test projectile. Projectile impact velocity was measured in front of the samples by the breaking of two printed, silver-circuit, thin paper screens set 0.5 meters (m) apart. A yaw card was positioned in front of each test sample to determine whether the projectile had a yaw

angle, if any, before it impacted the test samples. Tests were conducted at the United States Army Research Laboratory (ARL), Aberdeen Proving Ground, Maryland.

### **3.1.2 Test Samples**

Test samples were all of a ceramic composite laminate design. A typical construction for a composite laminate armor sample consist of a ceramic that is encapsulated using a fabric (Twaron®, Kevlar®, or Spectra Shield®) with one or more layers of different types of ballistic materials behind the ceramic material. Kevlar® and Twaron ® are tradenames for an aramid fiber, composed of aromatic polyamide and they provide exceptional impact resistance and tensile strength. Spectra Shield® is also a tradename for a high performance polyethylene (HPPE) fiber and it's impact resistance and tensile strength is greater than that of Kevlar® . The ceramic surface preparations, as well as a selection of adhesive and thermal treatments of the glued ceramics with the backing materials were optimized by the sample supplier. The detailed manufacturing process of each ceramic armor sample was not provided by the supplier because the information is proprietary. However, the usual process of fabricating a ceramic armor plate is by bonding solid particles of a ceramic into a monolithic structure (the plate), and compacting the particles into an approximate final shape. This process is known as sintering. Sintering, however, is just one part of the process, a process of densification that includes both solid-state and liquid phase sintering, transient liquid phase sintering, and reaction sintering to cause and control an increase in material density. Chemical vapor deposition (CVD) and hot pressing (HP) are two other types of densification processes. The type of processing used established

both the purity and the porosity of the material. Each of the test samples supplied had dimensions of 304 x 304 mm in size and different thickness. The areal densities of sample A, B, C, D, and E can not be provided in this study for security reasons. The test sample materials used in the experiment are listed in Table B-1<sup>2</sup>.

### **3.1.3 Test Projectile**

The projectile caliber that was used throughout the whole experimental test program was a 12.7 x 108 mm Armor Piercing Incendiary (API) round. This projectile was chosen based on a systems threat assessment for a United State Army weapon system which no longer exists, however, the threat projectile exists for other U.S Army weapon systems. The purpose of a system threat assessment is to assess the likely threat or threats that the weapon system would encounter. The results from the assessment were incorporated into the Operational Requirement Document for this particular weapon system.

Prior to conducting the experiments, a projectile velocity-propellant charge curve was determined for this weapon. The curve was required to provide a basis for selecting a powder charge to bullet weight ratio to achieve a desired ballistic impact velocity. A list of the projectile physical dimensions is provided in Table B-2 and the API round shown in Figure A-5.

### **3.1.4 Ballistic Test Procedure**

Before conducting firings of each sample, an estimate was made by the ARL test engineer, and by each technical advisor associated with each sample, of the projectile

---

<sup>2</sup> All tables are located in Appendix B

velocity that would result in a complete penetration of the sample materials. When the result yielded a complete penetration, the propellant charge for firing the second round was set equal to the powder charge of the first round, minus a propellant decrement that would give a 15 to 30 meters/second (m/s) velocity decrease in order to obtain a partial penetration. However, when the first round firings yielded a partial penetration, the propellant charge for second round was set equal to the first round plus a propellant increment for a 15 to 30 m/s velocity increase in order to achieve a complete penetration. The firings were continued until a  $V_{50}$  ballistic limit was determined. The  $V_{50}$  ballistic limit was determined by calculating the average velocity that resulted with an equal number of the highest partial and the lowest complete penetration impact velocities, within an allowable velocity span of 38 m/s. The reason for determining the  $V_{50}$  ballistic limit velocities for each sample material through ballistic testing is to evaluate, compare, and correlate the microstructure and mechanical properties of a selected group of ceramic armor samples to the  $V_{50}$  ballistic limit. The  $V_{50}$  ballistic limit is compared against the flexural strength, hardness, density, grain size, and porosity of each sample ceramic material. The microstructure and mechanical properties along with the  $V_{50}$  ballistic limit velocity is graphed to observe trends within the data that significantly influence the ballistic performance.

## **3.2 Sample Preparation for Characterization of Sample Physical Properties**

### **3.2.1 Ceramography Preparation**

In preparation for ceramography, samples were sectioned parallel to the thickness plane with a Buehler Isomet 1000 diamond saw. One set of samples was

mounted in a low viscosity epoxy that was infused under vacuum. The samples were polished in a five-step sequence using a Buehler Ecomet IV/Automet III polishing system. Four samples were chemically etched in Murkami's reagent and one sample was electrolytically etched with 1% potassium hydroxide (KOH) solution (Chinn, 2002). Ceramography protocol is described in detail in Appendix C.

### **3.2.2 Optical Micrograph**

Etched and unetched samples were observed and photographed with a Zeiss Axiovert 25CA optical metallograph. Unetched samples were used for porosity estimation. Representative areas were digitally photographed at 500x original magnifications and analyzed with an Image tool software package (PAX-it, 2001).

### **3.2.3 Scanning Electron Microscopy**

Etched samples were observed with a digital JEOL 5800LV Scanning Electron Microscope (SEM). Elemental analysis was done with an attached Oxford Link Isis Energy Dispersive X-ray Spectroscopy (EDS) system. Samples were surveyed at low and high magnification with representative areas digitally photographed.

### **3.2.4 X-Ray Diffraction**

Thin slices of each material were mounted onto x-ray sample holders. The X-Ray Diffraction (XRD) scans were performed using a Siemens (Bruker) D5005 X-ray diffractometer with Copper K alpha ( $\text{CuK}\alpha$ ) radiation. A basic search-match routine was run on each XRD plot to compare sample patterns to a Powder Diffraction File

(PDF) Database (ICDD, 2004). X-Ray Diffraction protocol is described in detail in Appendix C.

### 3.2.5 Flexure Testing

ASTM C-1161 (2002) was used as a guide for flexure testing. A diamond saw was used to trim samples to meet the “B” size sample dimensions for testing. Cut surfaces were smoothed on successive diamond wheels with 45 micrometer (μm) and 15 μm grit sizes. Testing was done in a 3-point bending mode. The samples of each material were loaded to failure. The failure load, P, was used in the flexure stress equation (ASTM C-1161, 20002) to determine the flexural strengths for a simply supported beam. This equation is given below:

$$\sigma = \frac{3PL}{2bt^2} \quad (3.1)$$

where,

$\sigma$  = Flexural Strength (MPa)

P = Breaking Load (kg)

L = Support Span (m)

b = Samples Width (m)

t = Samples Thickness (m)

Sample span was nominally 38.1 millimeters (mm) and the average width and thickness of the samples were respectively 5.08 mm and 4.064 mm. Flexure testing protocol is described in detail in Appendix C.



### **3.2.6 Microindentation Measurements**

Microindentation hardness measurements were performed by using an Instron Hardness Tester. ASTM C 1326 (2003) was used as a guide for microindentation hardness. A diamond pyramid indenter, with two  $136^\circ$  base angles and a required load of 500 grams (g), was applied to the SiC samples and a load of 1000 g was applied to the B<sub>4</sub>C sample. The hardness measurements were expressed as a Knoop hardness number (HK) (Chinn, 2002). The measurements were digitally displayed by the Instron Hardness tester. The microindentation measurements protocol is described in Appendix C. Note that ten (10) hardness measurements were made on a single test coupon of each material.

### **3.2.7 Density Measurements**

Density measurements were conducted by using a Micromeritics Accupyc 1330 Helium Pycnometer, which determines sample density by filling a sample chamber of 1 cubic centimeter (cc) with helium gas. The Micromeritics Accupyc 1330 Helium Pycnometer works by measuring the amount of displaced gas once a sample is inserted into the 1 cc volume. Once the displaced gas fills the sample chamber, the pressure is measured. The helium gas is then routed to a second empty chamber of the same volume and the pressure in both chambers is measured. The sample volume is calculated based on the pressures, and with the known weight of the sample, the density is then calculated. In preparation of the density measurements, portions of each of the five samples were cut to small cubes approximately 0.5 centimeter on a side, and

weighed to the nearest 0.0001 g. Density measurement protocol is described in detail in Appendix C.

## Chapter 4

### Results and Discussions

#### 4.1 Optical Micrographs

The objective of obtaining optical micrographs of each sample material surface was to observe and characterize the etched and unetched samples and determine their grain size and porosity. Figures A-6 and A-7 show the etched and unetched microstructures of the four SiC and one B<sub>4</sub>C ceramic samples analyzed. The microstructure of etched sample A in Figure A-6, etched with Murkami's reagent, revealed a microstructure consisting of coarser, elongated grains estimated at 6 microns. Figure A-7 of the unetched A sample shows a non-uniform distribution of porosity that is estimated at 5% based on a single tested sample. The microstructure of etched sample B in Figure A-6, etched with Murkami's reagent, revealed a fine grain structure estimated at 5 microns. Lighter grains were observed and presumed to be  $\beta$ -SiC that was not affected by the etchant. There were also micro cracks observed in the structure as shown in Figure A-6 (*See red arrow*). Figure A-7 of the unetched B sample shows a non-uniform distribution of porosity that is estimated at less than 2%, again based on only a single test coupon. The microstructure of etched sample C in Figure A-6, etched with Murkami's reagent, revealed a microstructure of mostly fine, equiaxed grains estimated at a mean size of 4 microns. The lighter colored grains were also coarser and were presumed to be  $\beta$ -SiC. Figure A-7 of the unetched C sample shows a non-uniform distribution of porosity that is estimated to be less than 5% in a single sample.

The microstructure of sample D in Figure A-6, etched with Murkami's reagent, revealed a microstructure consisting of equiaxed, recrystallized grains at approximately 6 microns. Figure A-7 of the unetched D sample shows small pores that were randomly distributed throughout the material and D is estimated to have a porosity less than 2% based on a single sample. The microstructure of sample E in Figure A-6, electrolytically etched with 1% KOH solution, revealed a microstructure consisting of equiaxed grains estimated at 15 microns. Figure A-7 of the unetched E sample shows a continuous network of micro pores throughout the section that is estimated to yield a porosity of 10% for a single sample. The grain size and porosity are plotted in Figure A-8 for the silicon carbide and boron carbide samples

## **4.2 Scanning Electron Microscopy**

The results of the SEM are presented in this paper to provide additional information concerning the microstructure features of the samples. Since the results relate to the qualitative features of the material, they were not used in correlation of the material microstructure parameters and mechanical properties with the ballistic limit. The results of the SEM micrographs at low and high magnification of the samples are shown in Figure A-9 and Figure A-10 respectively. The microstructure of sample A in Figure A-9 and Figure A-10 revealed a severe amount of relief from etching but there was no evidence at the grain nodes. Relief is a term used to describe the high-resolution and depth-of-field image of sample surface; it is an indication of the quality of a image, not an attribute of a microstructure. The microstructure of sample B in Figure A-9 and Figure A-10 revealed that the grains were not as distinct after etching. There was

significantly more of the white aluminum/yttrium deposit between grains. The microstructure of sample C Figure A-9 and Figure A-10 revealed relief in the bulk grain structure and some smoothing of pore walls which resulted from etching. There were small deposits of aluminum and yttrium detected between the grain boundaries. The microstructure of sample D in Figure A-9 and Figure A-10 revealed grains that were in sharp relief after etching. The white intergranular deposits contained aluminum but no yttrium. Finally, the microstructure of sample E in Figure A-9 and Figure A-10 revealed that the electrolytic etch fluid, KOH, selectively leached material at the grain boundaries. The white particles shown are aluminum-rich.

### **4.3 X-Ray Diffraction**

The X-ray diffraction (XRD) patterns of the samples were observed in detail, and compared to the standard Powder Diffraction File (PDF) Database (ICDD, 2004-2005). XRD plots of the sample ceramic materials are provided in Appendix D. The results are presented in this thesis to provide confirmation of the ceramics type.

Sample A had an XRD pattern that was similar to that of the C sample in that it was a close match with the 3C  $\beta$ -SiC phase, 6H crystal and other  $\alpha$ -SiC phases. The peaks from the trace phase were not as strong in the A material as they were in the C sample. Sample B had an XRD pattern that was very similar to that of sample C. The 3C, 6H and additional hexagonal phase of SiC were identified. There was more of the trace phase, possibly 4H SiC, detected in sample B than in C. For the C sample pattern, the closest matching pattern to the standard patterns were for the 3C cubic phase, which for silicon carbides is associated with  $\beta$ -SiC and  $\alpha$ -SiC hexagonal phases. One

hexagonal phase was identified as a 6H, the other was not identified. There was evidence of minor amounts of another SiC phase given by the small peaks near crystallographic directions of  $33.2^\circ$  and  $34.5^\circ$ . These peaks could not be positively identified due to their low intensity, but there were strong indications they were from the 4H  $\alpha$ -SiC phase. Sample D had an XRD pattern that was very similar to that of A, B and C. The 3C, 6H and additional hexagonal phase of SiC were present. Also, sample D had the most significant amount of the unidentified trace phase. Finally, the sample E XRD pattern did not match with any of the SiC phases. However, it was a very close match to the standard pattern for boron carbide ( $B_4C$ ). This data, coupled with the sample E density data positively identified sample E as boron carbide. There were no trace phases detected in the XRD pattern. In comparing peak positions and relative peak intensities, sample E was found to have an XRD pattern that was different from the other samples. The order and intensity of the three main sample E peaks between  $30^\circ$  and  $40^\circ$   $2\theta$  did not compare with the other sample patterns. There was also a series of smaller peaks that were not accounted for in the other sample patterns. This was a strong indication that the material was of a different composition. In summary, samples A, B, C, and D had very similar XRD patterns, all showing the presence of some trace phases in the patterns.

#### **4.4 Flexural Tests**

The reason for doing these test was because Lach (1993) and other ballisticians discovered that the flexural strength of a ceramic material seems to have a slightly greater influence on the ceramic's armor protection capability than its other mechanical

properties. The results of a series of structural failure test done on the ceramic samples in the present study were based on the 3 point bending, and the results of the tests are shown in Figure A-11. There were considerable scatter in the data from all samples. This was believed to be due, in part, to sample preparation and to internal flaws like cracks. The flexural strength data presented is not enough data to show general trends in mechanical behavior for correlation with the terminal ballistic behavior of the materials. There are too few data points to establish the average flexural strengths and their deviations within reasonable confidence limits or with much precision. According to ASTM C 1161 (2002) a minimum of ten samples is required for the purpose of estimating the average. Flexural strength for sample A ranged from 241 to 465 MPa. The B material flexural strength ranged from 402 to 633 MPa. The C material ranged from 312 to 656 MPa. The D material flexural strength ranged from 588 to 772 MPa, and finally the E material flexural strength ranged from 316 to 478 MPa. There were only two bending tests for sample E because of saw blade issues (breaking of the blades). Table 4.1 summarizes the results of the 3 point bending flexural tests and shows both the average failure strength as well as the standard deviation for each ceramic material. Figure A-12 is a bar chart based on Table B-3 showing the average and standard deviation.

#### **4.5 Microindentation Measurements**

As stated in the previous section, some ballisticians believe that flexural strength seems to have a slightly greater influence on ceramic armor protection capability than other mechanical properties. However, other ballisticians believe that hardness seems

to make a considerable contribution and to correlate best with the ceramic armor protective power. The results of series of microindentation hardness measurements of all the material are shown in Figure A-13. There are relatively small variations within the sample hardness of all the materials. The relatively small amount of the data is enough to establish the average hardness and their deviations within reasonable confidence limits or with acceptable precision. Hence, there is enough data to show general trends in mechanical behavior for correlation with the terminal ballistic behavior of the materials. According to ASTM C 1326 (2003) a least five and preferably ten indentations are required for hardness measurements. The hardness measurements for the silicon carbide samples (A, B, C, and D) ranged from approximately 2200 to 2450 kg/mm<sup>2</sup>. The boron carbide sample E hardness measurement ranged from 3125 to 3258 kg/mm<sup>2</sup>. Table B-4 summarizes the results of the microindentation measurements and shows both the average hardness as well as standard deviation for each ceramic material. Figure A-14 is a bar chart showing the averages and standard deviation.

#### **4.6 Density Measurements**

Density measurements are important to establish with accuracy for the measured samples that are in agreement with accepted published values for these types of materials. However, for armor application, density is most important because density should be low to reduce the weight of the armor. Densities for all of the ceramic materials except sample E fell within normal ranges for silicon carbide materials of 3.15 to 3.20 grams/cubic centimeter (g/cm<sup>3</sup>) (Ceradyne, Inc., 2003). There are enough data



points to establish the average densities and their deviations within reasonable confidence limits or with acceptable precision. The measured density of E was significantly lower than those of the other materials, and conformed more closely to that of boron carbide. The results are shown in Figure A-15. Table B-5 summarizes the results of the density measurements along with the averages and standard deviations. Figure A-16 is a bar chart showing the averages and standard deviations.

#### **4.7 Material Comparison**

It is of critical importance to know how, or to have a good estimate of how these materials are made. Materials and processes comprise one of several key technology areas within the Department of Defense which are essential for achieving the goals and objectives for the Army Technology Thrusts (Przemieniecki, 1993). The goals can be met by developing new material and process capabilities or exploiting materials produced by other countries. Exploiting material produced by other countries provides a direct and significant Research, Development, Test and Evaluation (RDE&T) cost saving.

The samples of ceramic ballistic armor provided by the foreign vendors were compared to SiC and B<sub>4</sub>C produced by three different processes by a United States company, Ceradyne, Inc (Ceradyne, Inc., 2003). From the results of the material analysis, each foreign sample was grouped in a category based on the measured sample compositions and properties. By comparing the properties of the foreign ceramics to materials produced by Ceradyne, Inc., samples B, C, D, and E are believed to have been processed by using a hot pressing; and sample A material is believed to have been

processed using a sintering process. Table B-6 provides the properties comparison of the foreign vendor's samples to that of ceramic produced by Ceradyne, Inc.

## **4.8 Ballistic Testing**

The ballistic tests are the most significant aspect of this research study because the results establish the  $V_{50}$  ballistic limit velocity, the velocity at which one-half of the tested projectiles will perforate the target and one-half will not, for modern ceramic armors. The  $V_{50}$  ballistic limit provides a statistical approximation to the projectile impact velocity at which complete penetration and incomplete penetration are equally likely to occur. The impact velocities for complete and partial penetration and the  $V_{50}$  velocity limits for each of the five samples are shown in Figure A-17 and summarized in Table B-6.

Also shown in Figure A-17 is the data for AISI 4340 armor steel provided as a baseline for comparing the ballistic performance of each of the ceramics (Mascianica, 1981). The first observation to be made from Figure A-17 is that the A sample shows a very high dispersion in its complete and partial penetration capability. It allowed a penetration to occur at the lowest recorded impact velocity, 209 m/s. It also has the lowest  $V_{50}$ , at 292 m/s. The best material with the smallest dispersion or scatter in its penetration characteristic, as well as the highest  $V_{50}$ , is the D material. Note that its  $V_{50}$  was 372 m/s, which was much better than that of the 4340 armor steel  $V_{50}$  of 310 m/s. All the other materials ballistic performance  $V_{50}$ 's are comparable in a range from 300 to 325 m/s, and have similar dispersion of penetration allowances. As a reminder, recall that the A material is believed to be manufactured from a sintered silicon carbide

material, and the D material appears to be a hot-pressed silicon carbide. Note also that the D material has higher flexural strength than the A material, Figure A-18, but an apparent lower Knoop hardness, Figure A-19. The data indicate that the E material, likely hot-pressed boron carbide, had flexural strength similar to the other silicon carbide materials that fell between the A and D performance limits but E is considerably harder, Figure A-19 and Table B-4. On the other hand, B and C have essentially the same flexural strength, density, and hardness as the A material, see Table B-4. Therefore, the success of the D material, compared to the A, B, and C must lie in the details of its manufacturing process. D's micrographs (Figures A-9 and A-10) do not appear fundamentally different from the micrographs of B, C, and E.

#### **4.9 Material and Microstructure Properties vs. $V_{50}$ Ballistic Limit**

In an attempt to correlate the ballistic performance of the ceramic armor samples to their material properties, a series of figures were prepared. Figures A-18 through A-22 provides the  $V_{50}$  ballistic limit for each of the ceramic samples compared to the different microstructure and the mechanical properties of each material. Again, the intent of these charts is to identify correlation between the microstructure and the mechanical properties to the ballistic performance, and to identify those material properties that are necessary to achieve a high ballistic performance based on a known or hypothesized manufacturing process. As stated previously, it is clear that the ballistic performance of the D material is well correlated with its flexural strength, which is the highest of all the materials shown in Figure A-18. Figure A-19 shows that hardness does not appear to correlate with ballistic effectiveness, since materials A, B,

C, and D all appear to have the same hardness. The E material appears to have a significantly higher hardness than D, but its  $V_{50}$  performance is lower.

Figure A-20 compares material density to  $V_{50}$  performance and shows that density does not appear to correlate with ballistic performance. Materials A, B, C, and D all have about the same density, with E having a slightly lower density.

Figure A-21 compares mean measured material grain size to  $V_{50}$  ballistic performance. Again, there is no apparent correlation of  $V_{50}$  performance with grain size observed. Nor can the dispersion of the A results be related to grain size.

Finally, Figure A-22 compares material estimated porosity to  $V_{50}$  ballistic performance. Comparing Figure A-17 and A-22, there does seem to be somewhat of a correlation between increased porosity levels and ballistic performance data dispersion or scatter, the less porous B and D do appear to have less data scatter and smaller porosity than A and C. Yet, porosity can't completely explain ballistic limit velocity scatter because E material has a relatively small amount of  $V_{50}$  dispersion, but also has the highest estimated porosity. Therefore, porosity and manufacturing details or process apparently have intertwined roles in establishing the  $V_{50}$  ballistic performance of the ceramic materials. More research along these lines is definitely required to establish the best combination of materials and processing to establish the highest possible  $V_{50}$  ballistic performance, along with a high level of consistent performance. Also shown in Figure A-18 through A-22 are the yield strength (Air Force Materials Laboratory, 1964), hardness (MatWeb, 1996-2005), density (MatWeb, 1996-2005), grain size (Air Force Materials Laboratory, 1964), and porosity (Military Specification -

5000E, 1982) for AISI 4340 armor steel provided as a baseline for comparing the ballistic performance of each of the ceramics.



## **Chapter 5**

### **Conclusion**

It was found that the ballistic velocity limit of the foreign ceramic materials increased as their flexural strength increased. Therefore ballistic limit protection of a ceramic material appears well correlated with its flexural strength. Other materials properties such as density, microindentation hardness, and grain size may be important in determining the ballistic performance but do not directly correlate with the ballistic performance. The porosity data does seem to show correlation between increased porosity levels and ballistic performance data dispersion or scatter. As stated by Medvedovski (2002) no single property appears to have a direct correlation with ballistic performance, because the fracture mechanism during bullet impact is complicated, and the crack formation and material rupture is caused by various stress factors. Crack formation and rupture occurs in an extremely short time.





## **Chapter 6**

### **Recommendations**

Future work is needed in order to determine more accurately the correlation between the ballistic limit velocity and the flexural strength. Other areas of study that are worth investigating are the effects of different grain size (sub- $\mu\text{m}$ ), and lower volume fraction (porosity), and manufacturing process on  $V_{50}$  ballistic limit performance of ceramic armors, and more samples need to be tested to improve confidence of results obtained



## List of Reference

Adams, J. W., Gilde, G. A., Burkins, M., and Franks L. (2001). Microstructure Development of Aluminum/Titanium Diboride Composite for Penetration Resistance. *Proceedings of the Ceramic Armor Materials by Design Symposium held at the Pac Rim IV International Conference on Advanced Ceramics and Glass, November 4-8, 2001 in Wailea, Maui, Hawaii*. Ed. James W. McCauley, Andrew Crowson, William A. Gooch, jr., A. M. Rajendran, Stephan J. Bless, Karhryn V. Logan, Michael Normandia, and Steven Wax: The American Ceramic Society, 2002. pages 629-634.

Air Force Materials Laboratory (1964). Investigation of the Effects of Stress Corrosion on High-Strength Steel Alloys. *Air Force Material Laboratory, Research and Technology Division, Air Force System Command, Wright-Patterson Air Force Base, Ohio*, ML-TDR-64-3, February 1964.

Amos, C. W. (1990). Lightweight Armor Design Handbook-Monolithic Armor. *U.S. Army Laboratory Command*, MTL-TR-90-40, August 1990.

ASTM C-1161 (2002). Standard Test Method for Flexural Strength of Advanced Ceramics at Ambient Temperature. *ASTM International*. 2002.

ASTM C-1326 (2003). Standard Test Method for Knoop Indentation Hardness of Advanced Ceramics. *ASTM International*. 2003.

Bartkowski, P., and Spletzer, S. (2001). Porosity Effects on the Elastic Constants of Five Varieties of Silicon Carbide Ceramic. *Army Research Laboratory*, ARL-TR-2606, November 2001.

Ceradyne, Inc (2003). Ceradyne's Boron Carbide and Silicon Carbide Ceramic: Property Comparison. *Ceradyne, Inc, 3169 Redhill Costa Mesa, CA 92626*, 2003.

Chinn, R. E. (2002). Ceramography: Preparation and Analysis of Ceramic Microstructures. *ASM International*, 2002.

ICDD (2004-2005). Powder Diffraction File and Related Products. *The International Centre for Diffraction Data*, 2004-2005.

Faber, K. S., and Meyer, L. W. (1995). Correlation between the Mechanical Data of Ceramics and Their Protective Power against Impact Loading. Final Report EB 6/95 (Part 3), Technical University Chemnitz-Zwickau, *Department of Engineering Materials*.

Krell, A., and Blank, P. (1995). Grain Size Dependence of Hardness in Dense Submicrometer Alumina. *Journal of American Ceramic Society*, Volume 78, No. 4, pages 1118-1120.

Krell, A., Strassburger, E., and Lexow, B., Ceramic Armor with Submicron Alumina against Armor Piercing Projectiles. *Proceedings of the Ceramic Armor Materials by Design Symposium held at the Pac Rim IV International Conference on Advanced Ceramics and Glass, November 4-8, 2001 in Wailea, Maui, Hawaii*. Ed. James W. McCauley, Andrew Crowson, William A. Gooch, jr., A. M. Rajendran, Stephan J. Bless, Karhryn V. Logan, Michael Normandia, and Steven Wax: The American Ceramic Society, pages 83-90.

Lach, E. (1993). Mechanical Behavior of Ceramic and their Ballistic Properties. *Cfi/Beer*. DGK 70 (1993) No. 9, pages 486-490.

Mascianica, F. (1981). Ballistic Technology of Lightweight Armor. AMMRC-TR-81-20

Matchen, B. (1996). Application of Ceramics in Armor Products. *Engineering Materials*, Volumes 122-124, pages 333-342.

MatWeb (1996-2005). Material Properties Data. <http://www.matweb.com>, 4/01/2005.

Medvedovski, E. (2002). Alumina Ceramics for Ballistic Protection. *American Ceramic Society Bulletin*, Volume 81, No. 4, pages 45-50.

Military Standard (1997). Department of Defense Test Method Standard, V<sub>50</sub> Ballistic Test for Armor. *Department of Defense*. MIL-STD-666F,

Military Specification (1982). Steel, Chrome-Nickel-Molybdenum (E4340) Bars and Reforging Stock. *Department of Defense*. Mil-S-5000E.

PAX-it (2001). Imaging System for Science and Industry. *MIS, West Grand Avenue, Franklin, Park, IL*, Version 3.2, 2001.

Przemienicki, J. S. (1993). Acquisition of Defense Systems. *American Institute of Aeronautics and Astronautics, Inc*, 1993.

Rozenberg, Z. and Yeshurun, Y. (1988). The Relation between Ballistic Efficiency and Compressive Strength of Ceramic Tiles. *International Journal of Impact Engineering*, Volume 7, No 3, pages 357-362.



## **Appendices**







Figure A-1: Performance of Models A, B, and C

## Appendix A

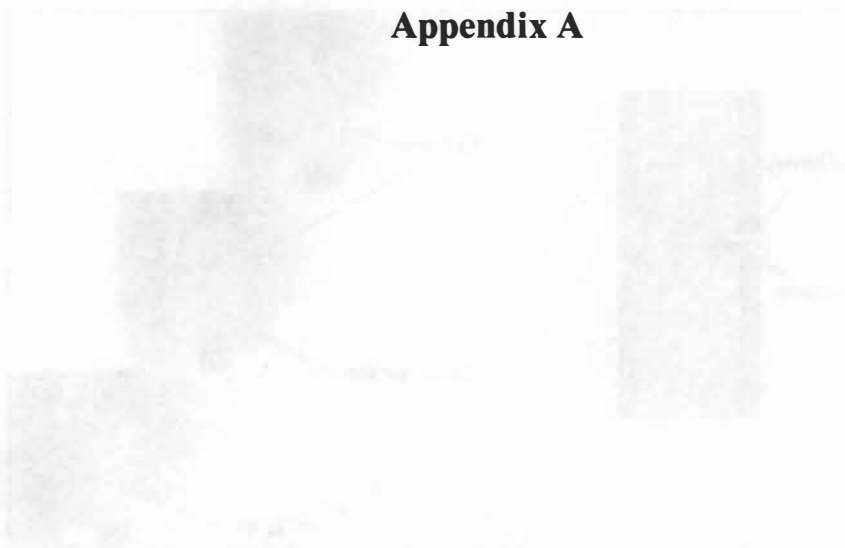
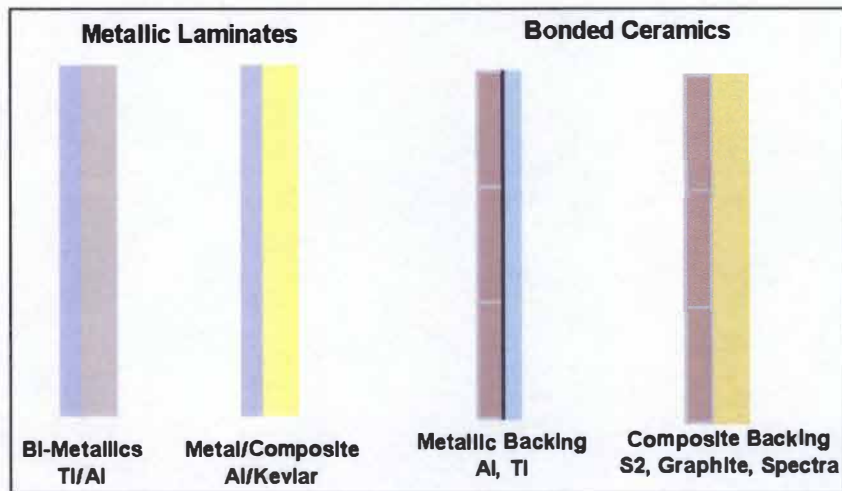
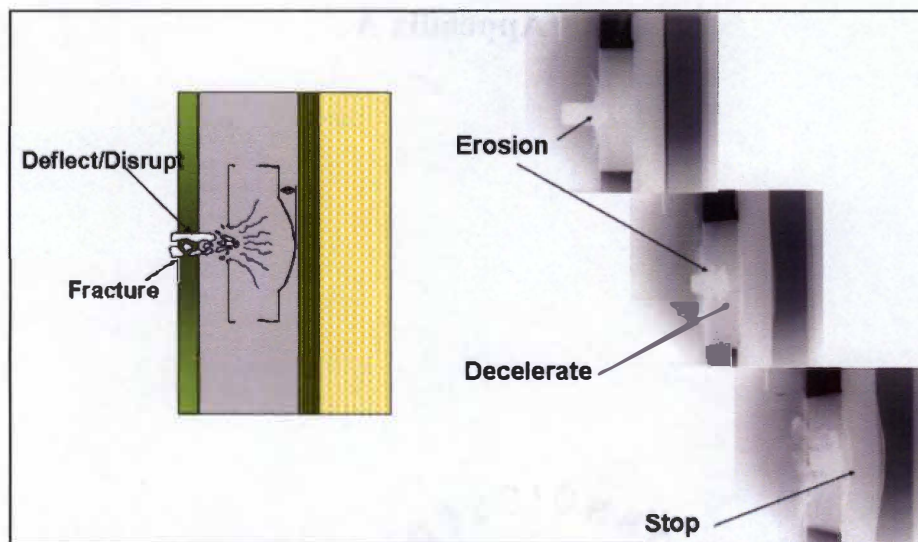


Figure A-2: Performance of Models A, B, and C



**Figure A-1: Laminated Armor Options**



**Figure A-2: Penetrator Defeat Mechanism**

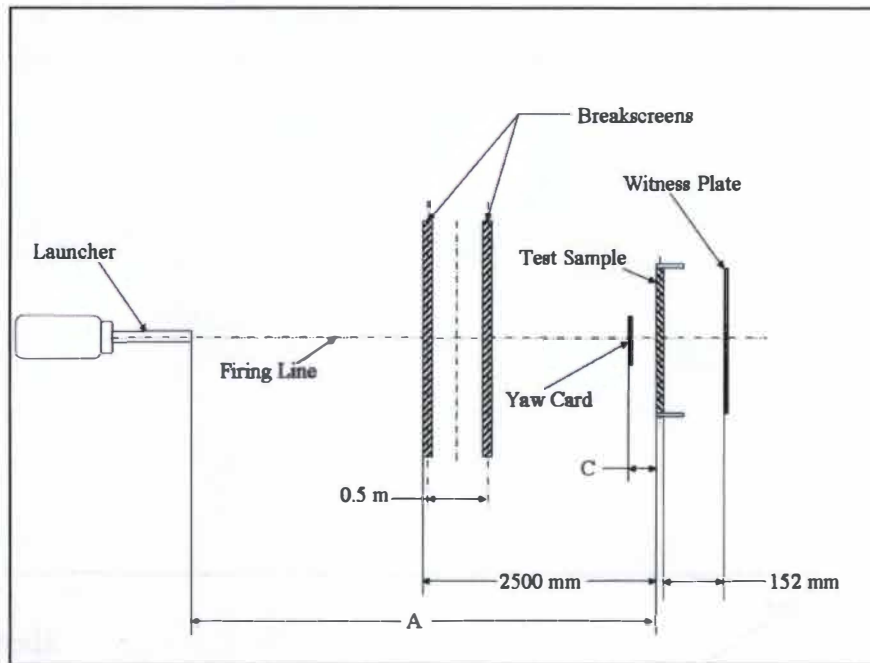


**Figure A-3: Illustration of Ballistic Test Setup**

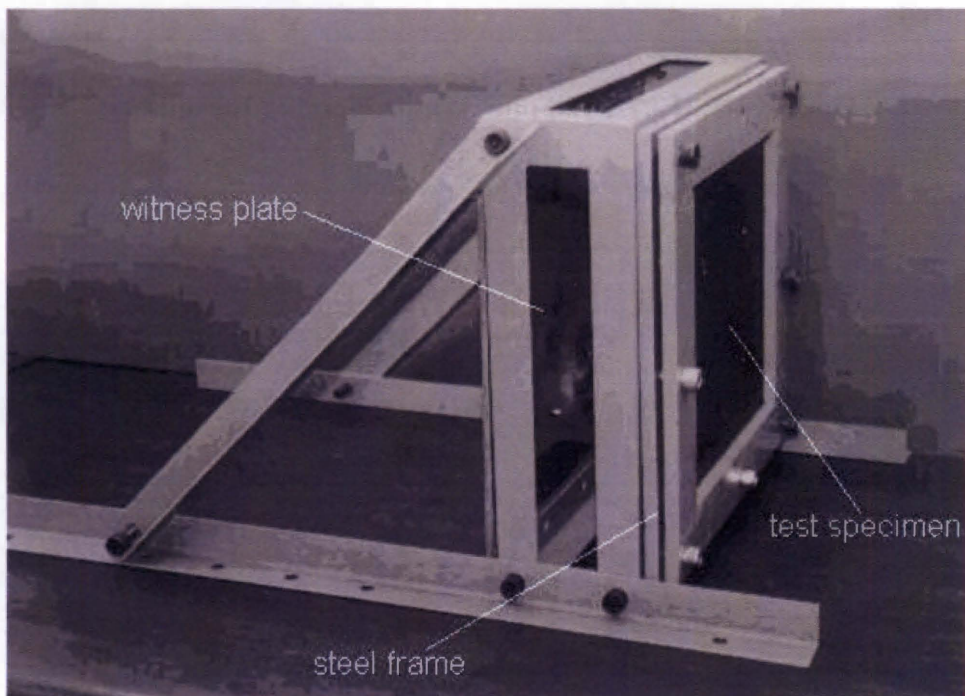


**Figure A-4: Steel Frame Mounting Bracket**

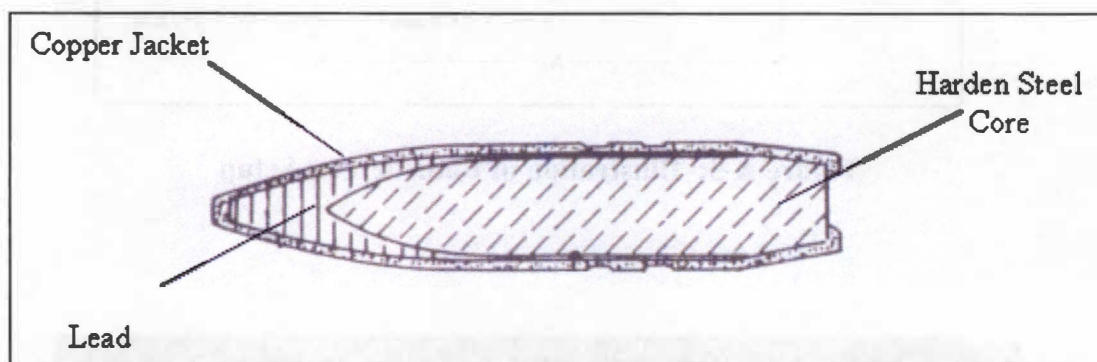


**Figure A-5: 12.7 x 108 mm Armor Piercing Incendiary**

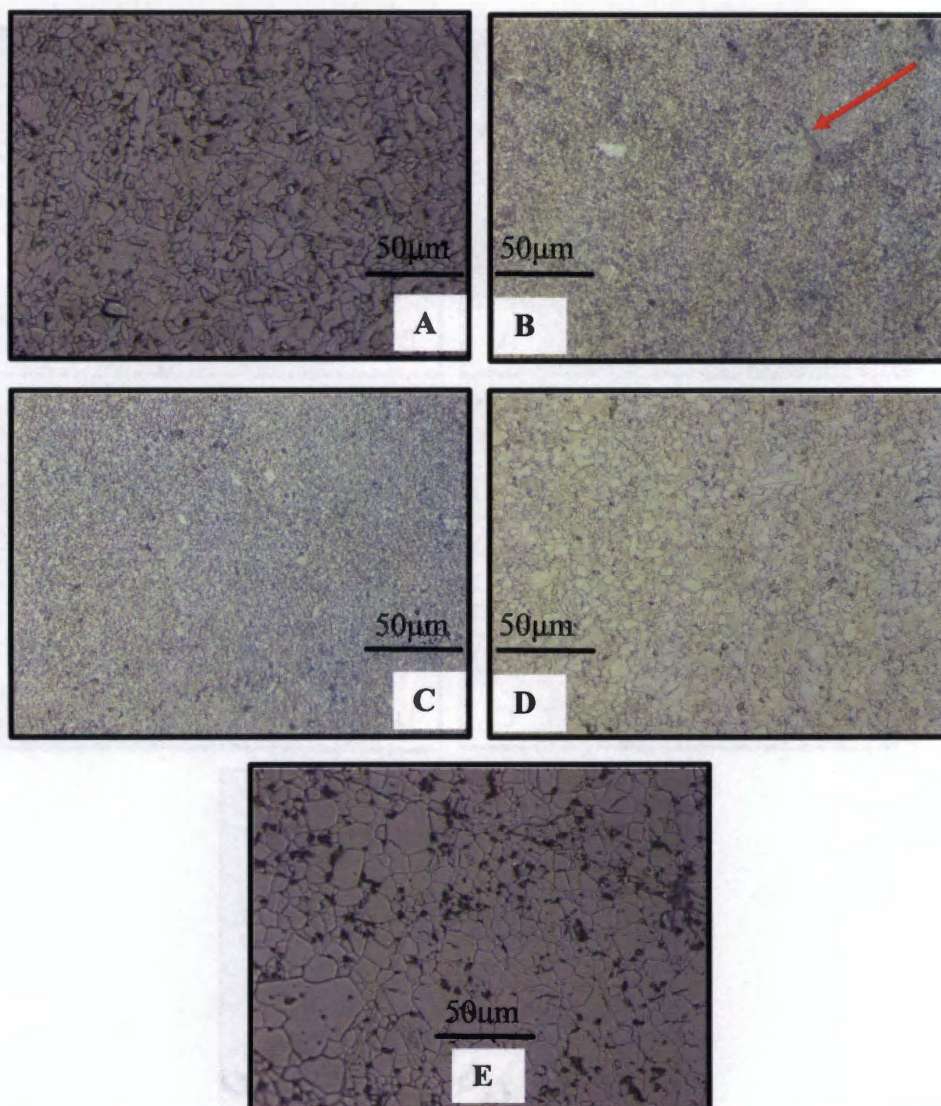


**Figure A-6: Etched Microstructures of Ceramic Materials Analyzed**



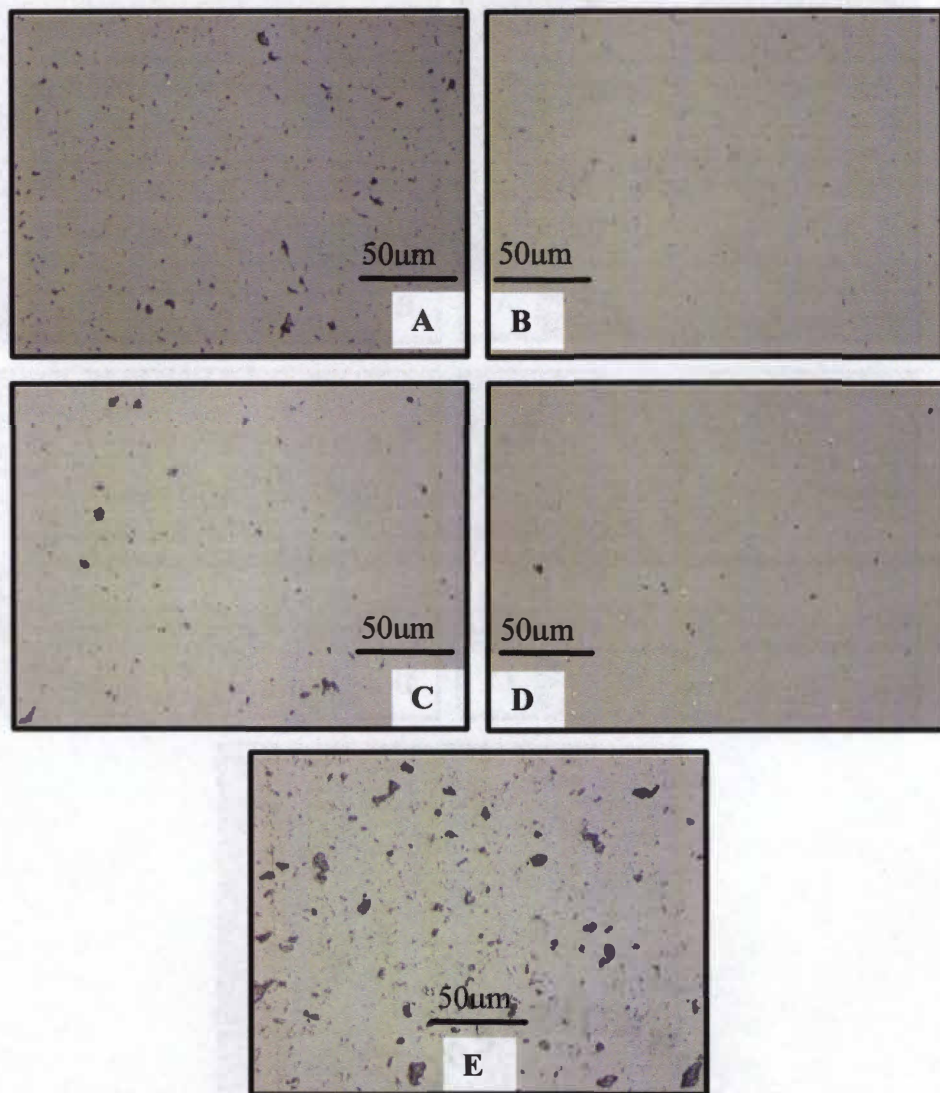


**Figure A-7: Unetched Microstructures of Ceramic Materials Analyzed**

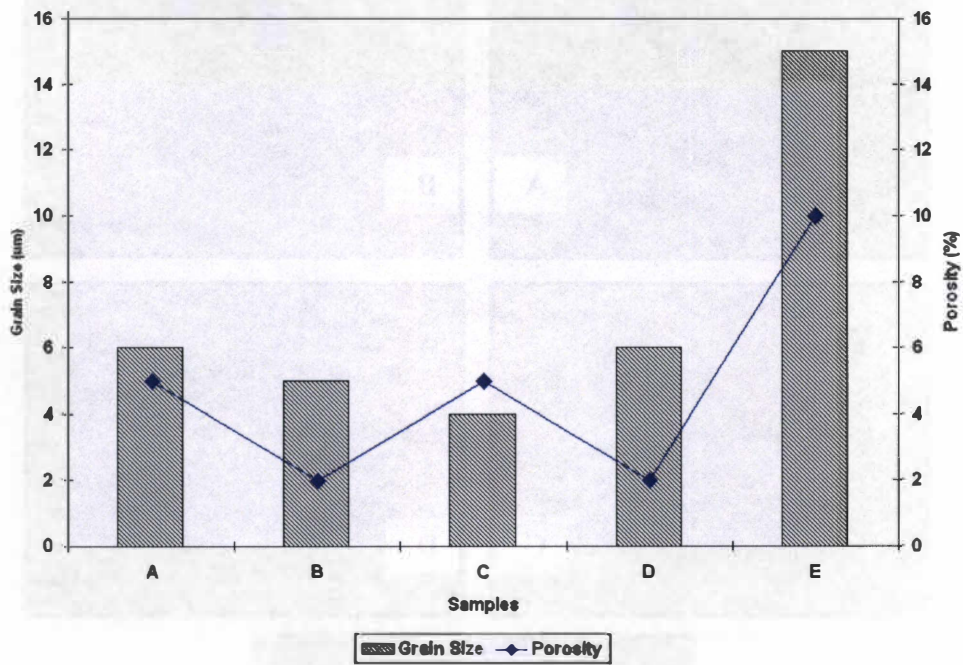


**Figure A-8: Grain Size and Porosity of Samples**

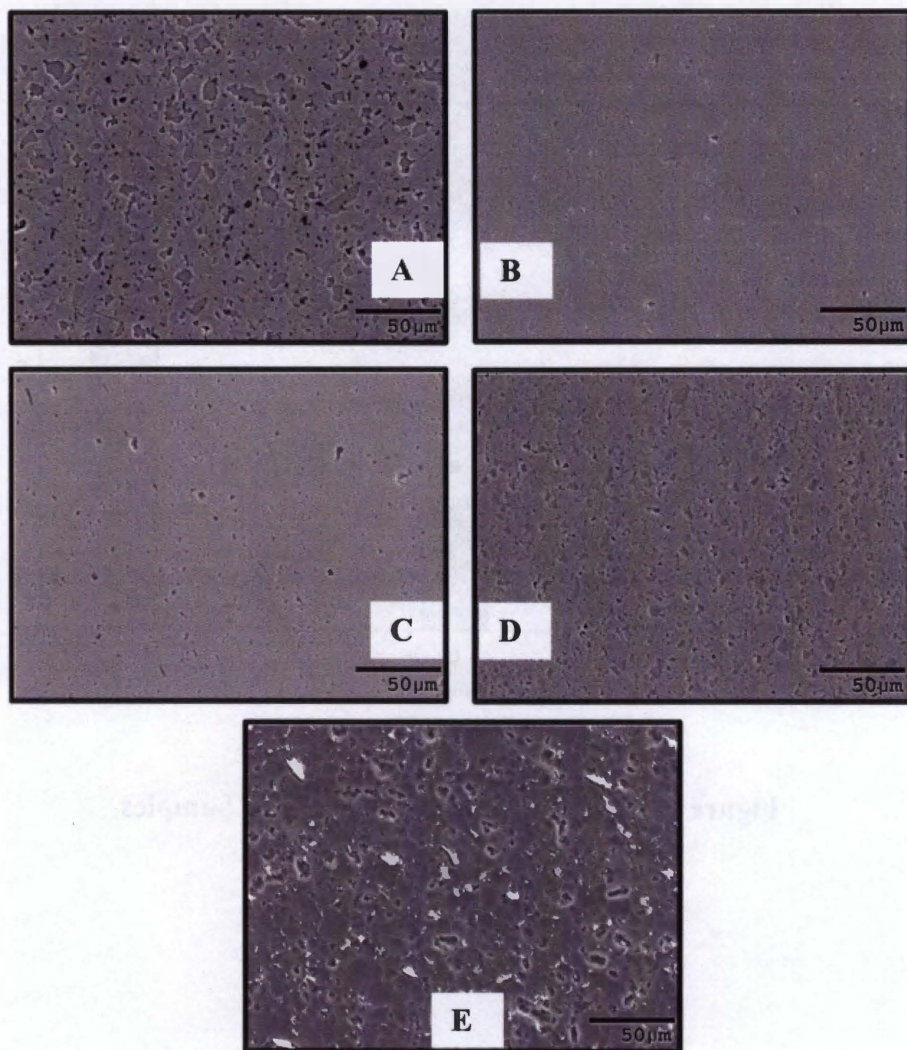


**Figure A-9: Scanning Electron Microscopy of Materials Analyzed at 500x**



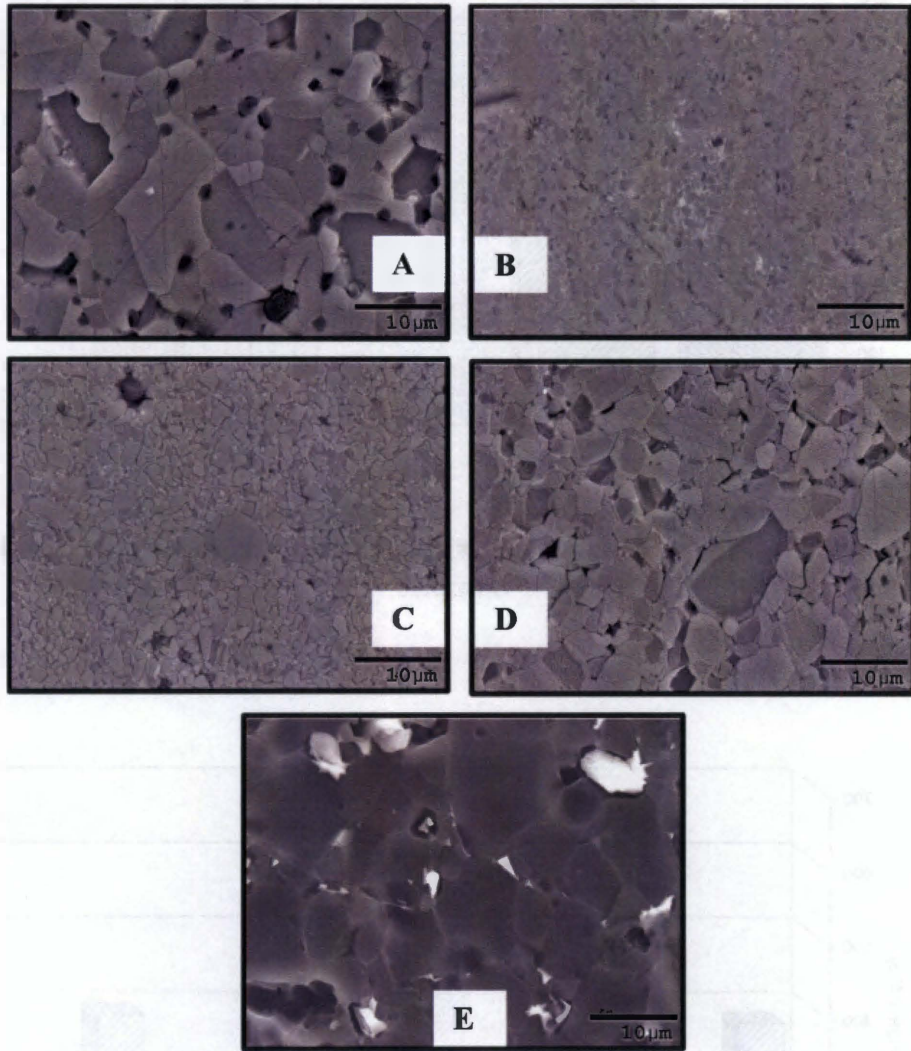


**Figure A-10: Scanning Electron Microscopy of Materials Analyzed at 2500x**

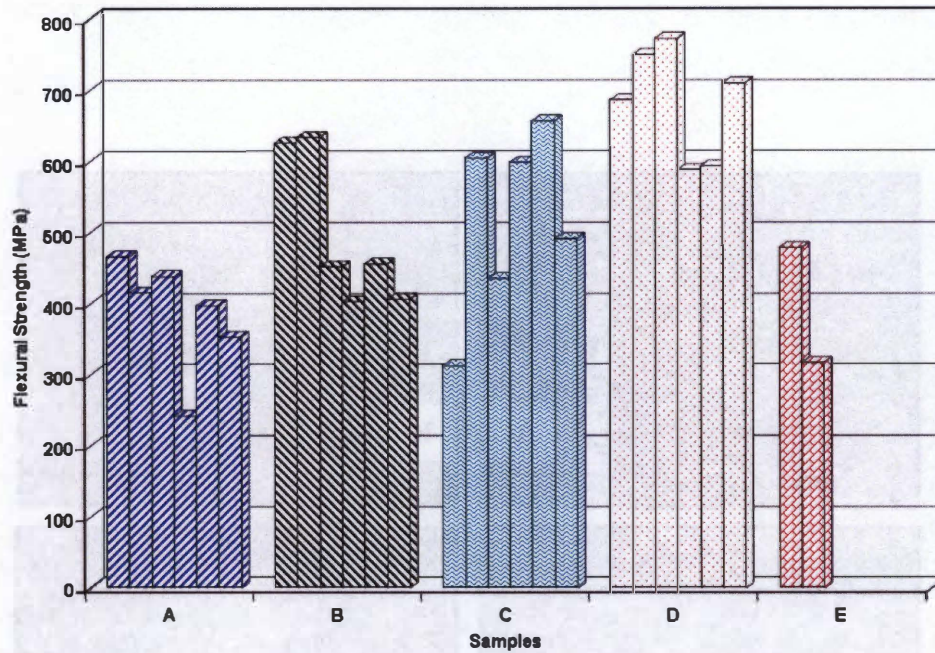


**Figure A-11: Flexural Strength (at brittle fracture) from 3-Point Bending of Samples**

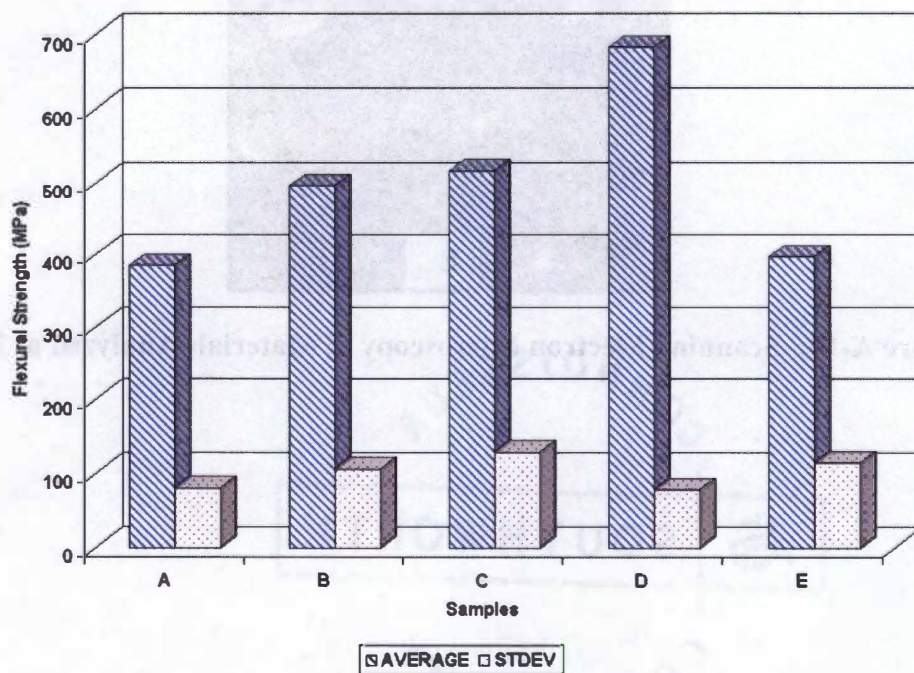


**Figure A-12: Statistical Analysis of Samples Flexural Strength**



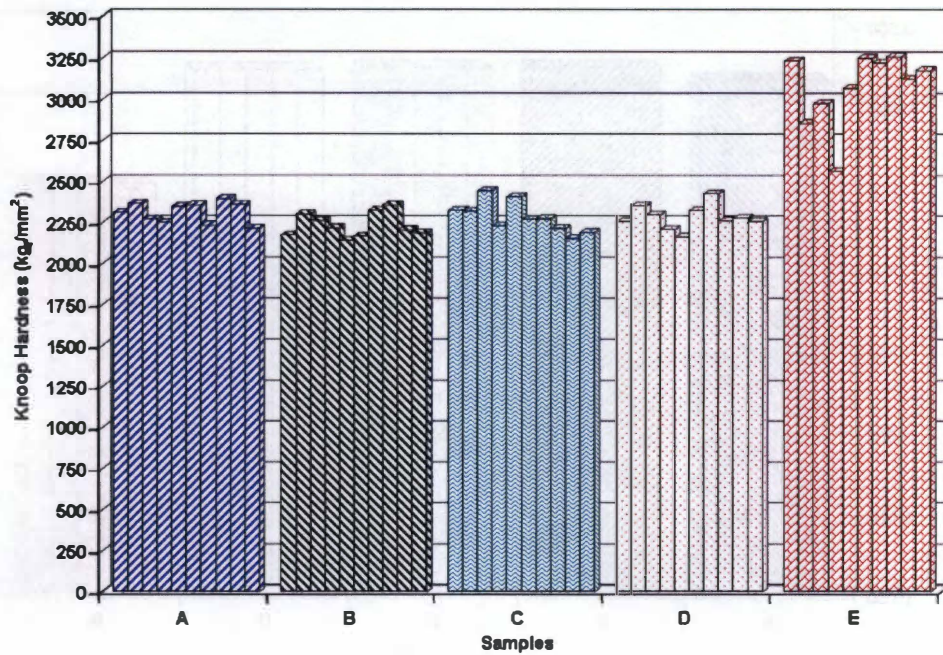


**Figure A-13: Microindentation Hardness of Samples**

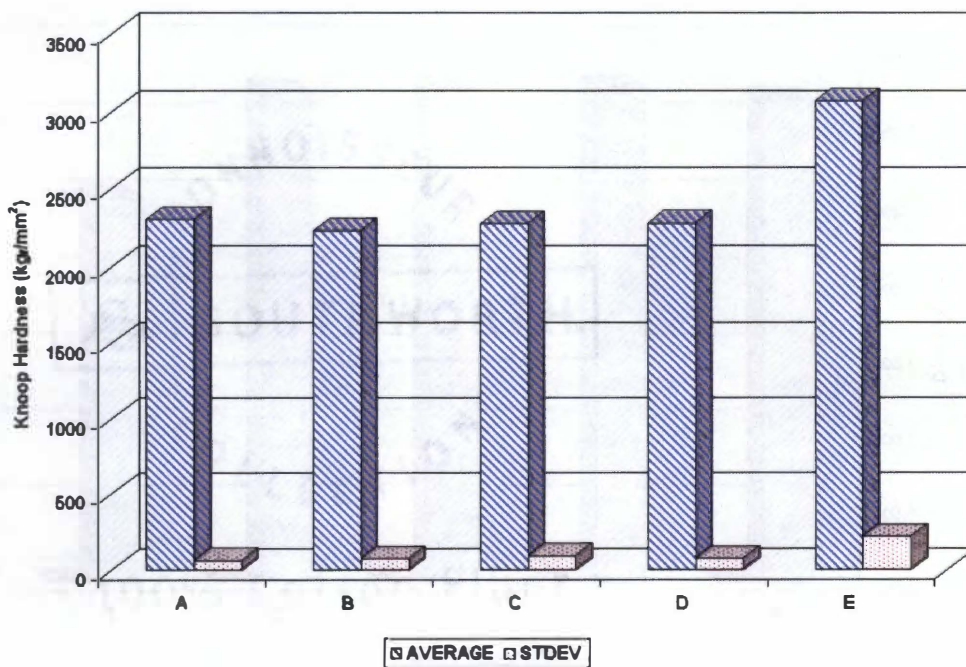


**Figure A-14: Statistical Analysis of Samples Microindentation Hardness**

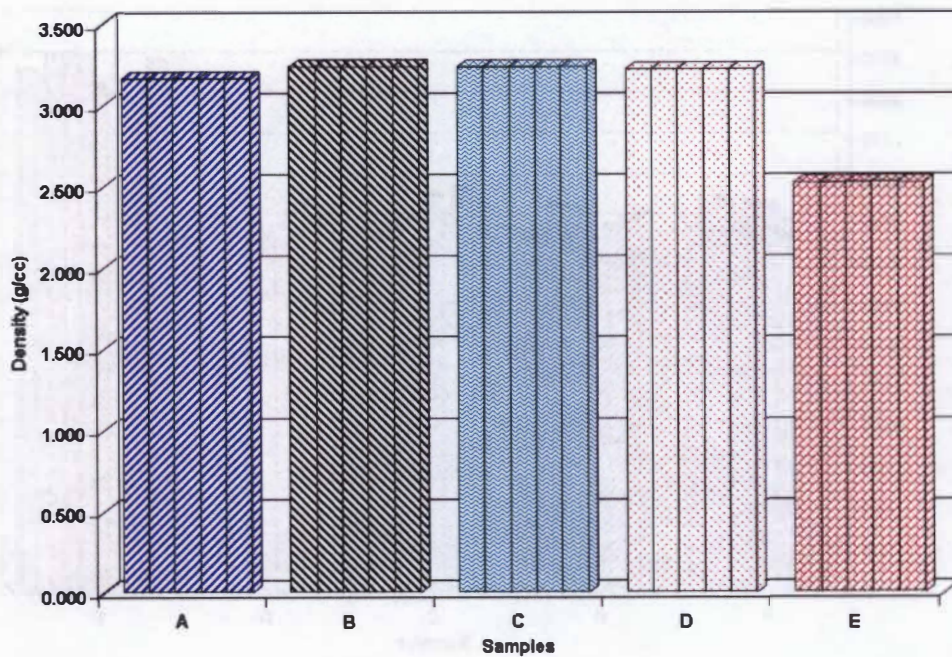


**Figure A-15: Density Measurement of Samples**

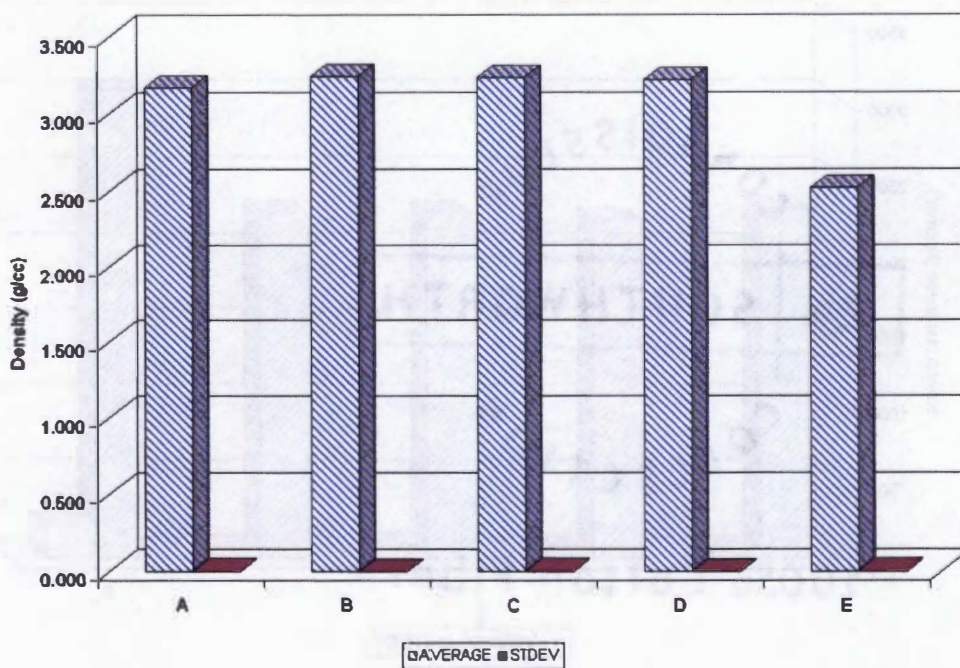


**Figure A-16: Statistical Analysis of Samples Density**



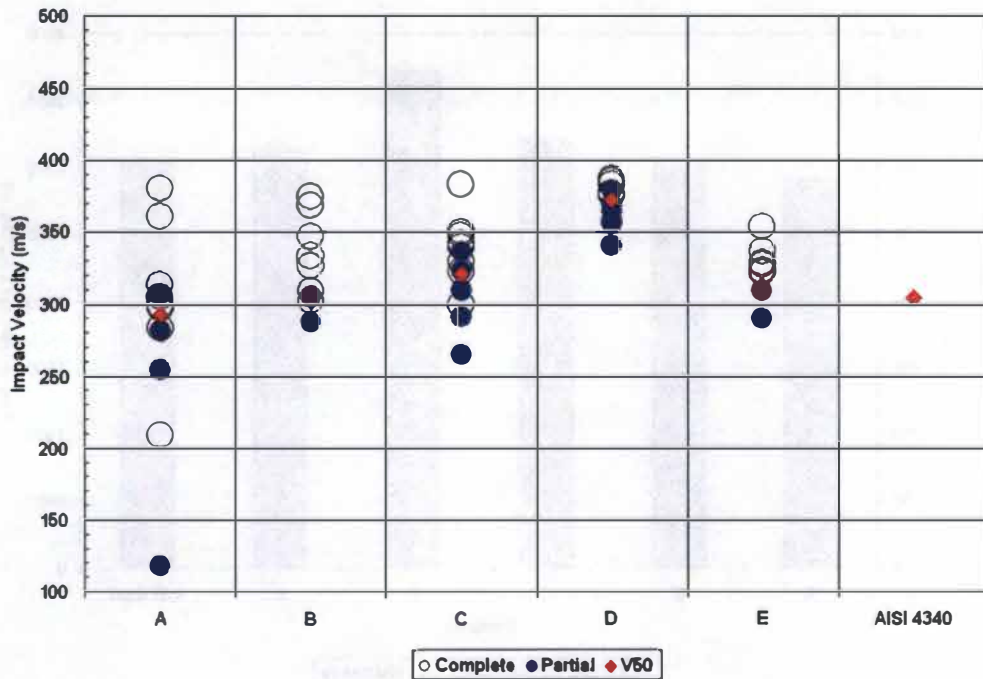


Figure A-17: Single Shot Ballistic Results of Ceramic Samples

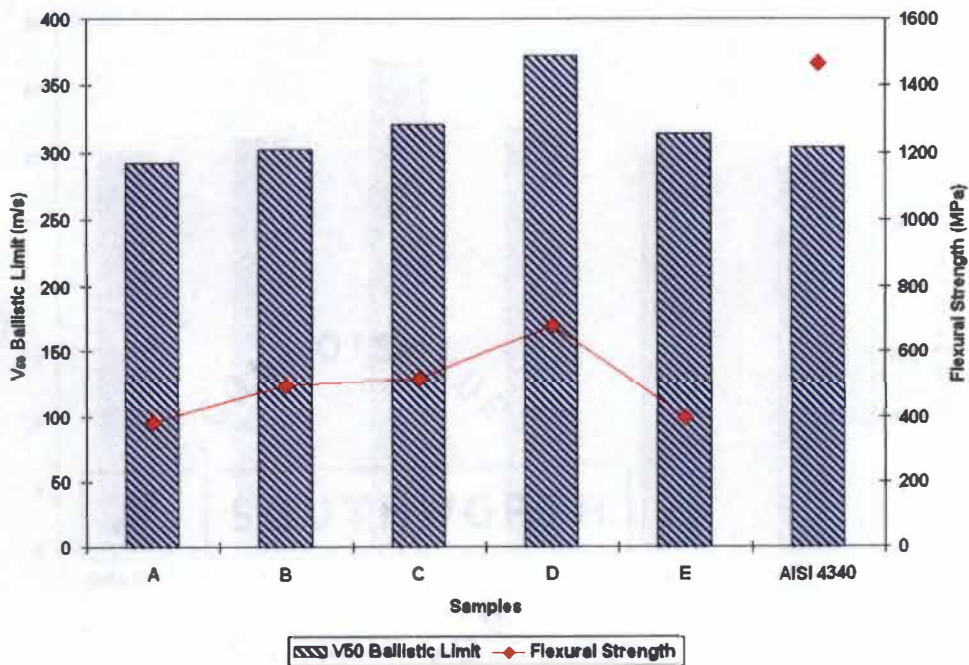
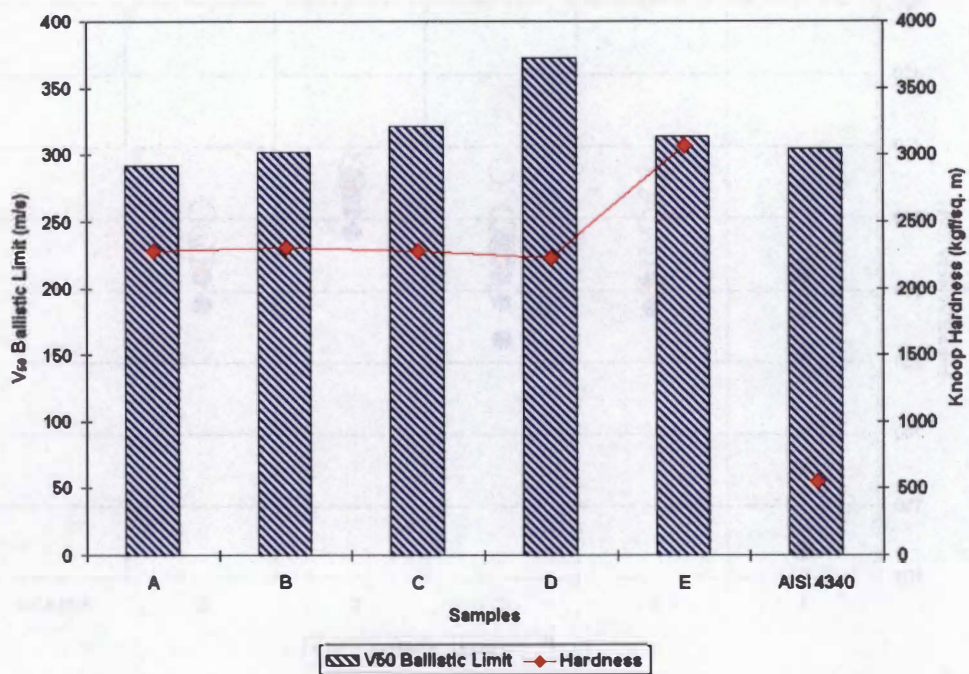
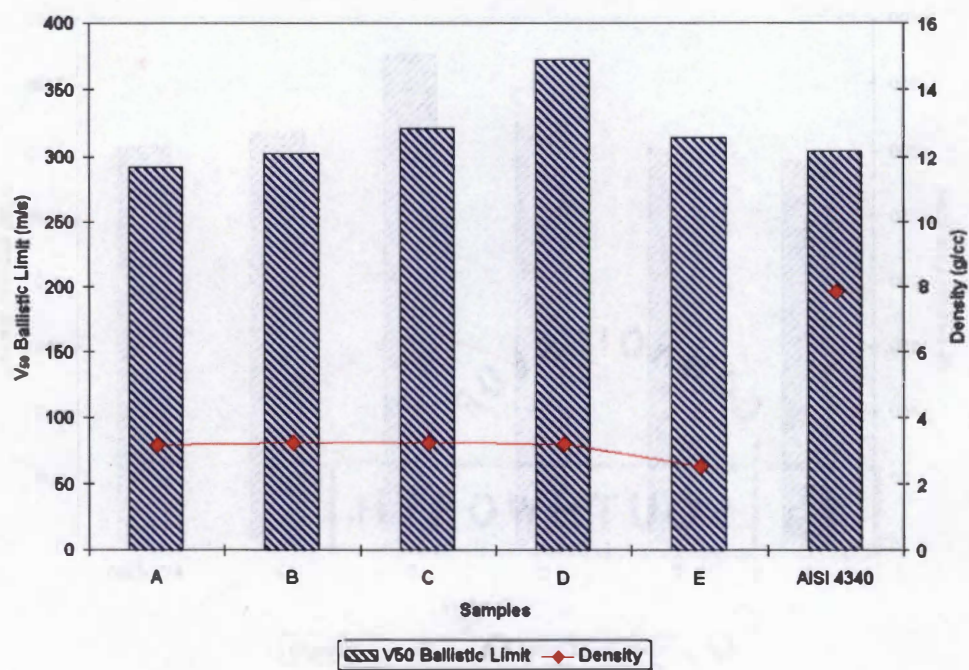


Figure A-18:  $V_{50}$  Ballistic Limit Velocity and Flexural Strength



**Figure A-19: V<sub>50</sub> Ballistic Limit Velocity and Knoop Hardness**



**Figure A-20: V<sub>50</sub> Ballistic Limit Velocity and Density**

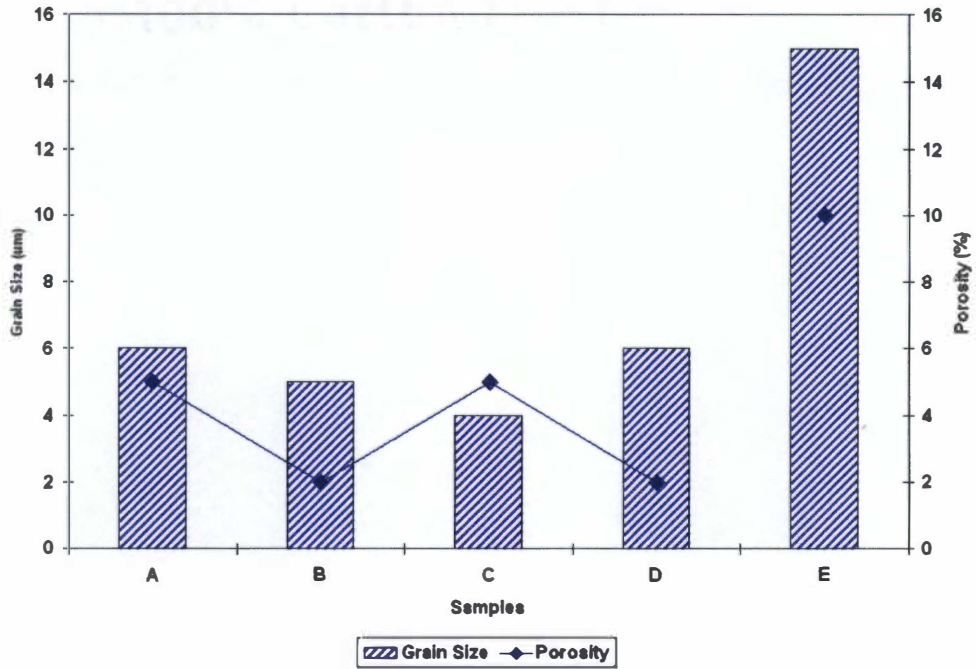


**Figure A-21:  $V_{50}$  Ballistic Limit Velocity and Grain Size**

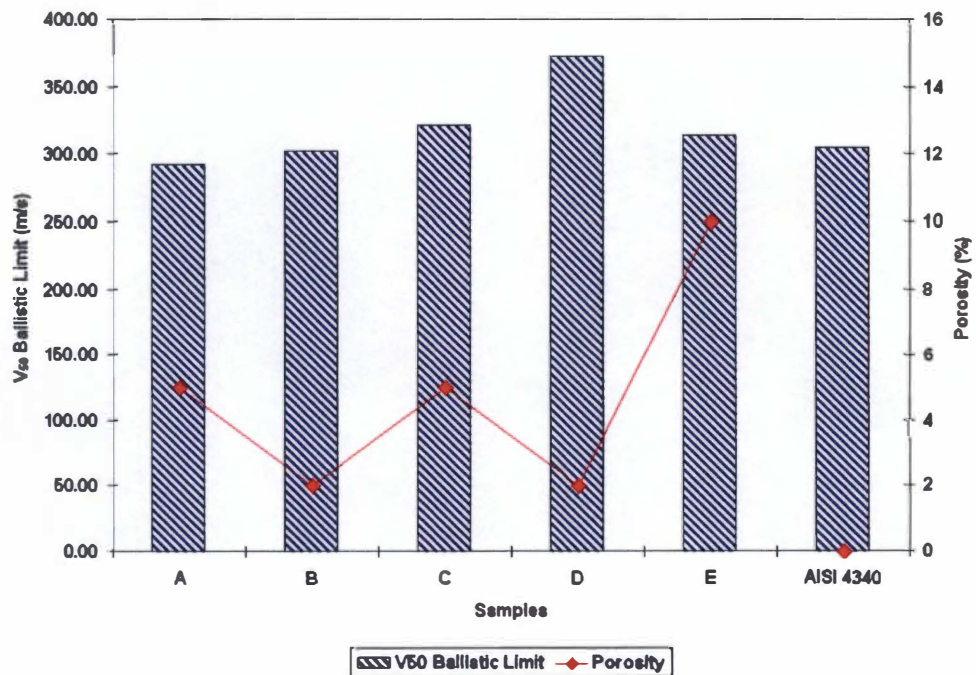


**Figure A-22:  $V_{50}$  Ballistic Limit Velocity and Porosity**





Table B-1: Properties of Common Composite Reinforcing Materials

Material	Modulus of Elasticity (ksi)	Tensile Strength (ksi)	Weight (lb/ft <sup>3</sup> )
Carbon Fiber	140,000	175,000	140
Kevlar Fiber	110,000	170,000	130
Fiberglass	10,000	100,000	160
Basalt Fiber	10,000	100,000	160
Carbon Fiber (Random)	140,000	175,000	140
Kevlar Fiber (Random)	110,000	170,000	130
Fiberglass (Random)	10,000	100,000	160
Basalt Fiber (Random)	10,000	100,000	160

Table B-2: Properties of Common Composite Reinforcing Materials

Material	Modulus of Elasticity (ksi)	Tensile Strength (ksi)	Weight (lb/ft <sup>3</sup> )
Carbon Fiber	140,000	175,000	140
Kevlar Fiber	110,000	170,000	130
Fiberglass	10,000	100,000	160
Basalt Fiber	10,000	100,000	160
Carbon Fiber (Random)	140,000	175,000	140
Kevlar Fiber (Random)	110,000	170,000	130
Fiberglass (Random)	10,000	100,000	160
Basalt Fiber (Random)	10,000	100,000	160

## Appendix B

Table B-3: Properties of Common Composite Reinforcing Materials

Material	Modulus of Elasticity (ksi)	Tensile Strength (ksi)	Weight (lb/ft <sup>3</sup> )
Carbon Fiber	140,000	175,000	140
Kevlar Fiber	110,000	170,000	130
Fiberglass	10,000	100,000	160
Basalt Fiber	10,000	100,000	160
Carbon Fiber (Random)	140,000	175,000	140
Kevlar Fiber (Random)	110,000	170,000	130
Fiberglass (Random)	10,000	100,000	160
Basalt Fiber (Random)	10,000	100,000	160

**Table B-1: Summary of Ceramic Composite Ballistic Materials**

Samples	Panels Description
A	Polycarbonate/Silicon Carbide/Carbon/ Spectra Shield/Kevlar
B	Carbon/Silicon Carbide/Twaron
C	Twaron/Silicon Carbide/Twaron
D	Twaron/Silicon Carbide/Twaron
E	Kevlar/Boron Carbide/Kevlar

**Table B-2: Summary of Projectile Physical Dimension**

Projectile			Core/Penetrator			
Length (mm)	Diameter (mm)	Weight (grains)	Material	Length (mm)	Diameter (mm)	Weight (grains)
64.516	12.979	745	Steel	52.578	10.846	464
			Lead			105

Source: Amos, 1990

**Table B-3: Summary of 3-Point Bending Flexural Strength (MPa)**

A	B	C	D	E
466	626	313	686	478
415	633	604	750	317
438	452	435	772	
241	402	598	588	
397	455	657	593	
352	406	491	709	
		<b>AVERAGE</b>		
385	496	516	683	397
		<b>STDEV</b>		
± 80	± 106	± 129	± 78	± 114

**Table B-4: Summary of Microindentation Hardness Measurements ( $\text{kg}/\text{mm}^2$ )**

A	B	C	D	E
2310	2174	2326	2257	3233
2365	2301	2318	2352	2855
2269	2261	2444	2297	2976
2249	2217	2229	2209	2564
2348	2141	2408	2163	3068
2356	2167	2269	2326	3249
2233	2326	2273	2426	3221
2395	2356	2213	2261	3258
2360	2205	2152	2277	3125
2213	2186	2190	2257	3176
		<b>AVERAGE</b>		
2310	2233	2282	2283	3073
		<b>STDEV</b>		
$\pm 64$	$\pm 74$	$\pm 93$	$\pm 74$	$\pm 222$

**Table B-5: Summary of Density Measurements ( $\text{g}/\text{cm}^3$ )**

A	B	C	D	E
3.1654	3.2377	3.2366	3.2206	2.5212
3.1655	3.2376	3.2363	3.2206	2.5205
3.1666	3.2373	3.2357	3.2200	2.5216
3.1660	3.2375	3.2348	3.2205	2.5232
3.1662	3.2377	3.2367	3.2202	2.5209
		<b>AVERAGE</b>		
3.1659	3.2376	3.2360	3.2204	2.5215
		<b>STDEV</b>		
$\pm 0.0005$	$\pm 0.0002$	$\pm 0.0008$	$\pm 0.0003$	$\pm 0.0010$

**Table B-6: Ceradyne's Silicon Carbide and Boron Carbide Ceramic Property**

Process	Hot Pressing (SiC)	Sintering (SiC)	Hot Pressing (B4C)
Purity	98.5%	95%	>98.5%
Density	3.20	3.20	2.5
Flexural Strength	634	400	410
Knoop Hardness	2300	2600	3200
Samples	B, C, & E	A	E

Source: Ceradyne, Inc., 2003

**Table B-7: Single Shots Ballistic Results of the Ceramic Opaque Composite Armors**

Samples	Velocity (m/s)	P/C	V <sub>50</sub> (m/s)	Spread (m/s)
A	381	C	292 a	24
A	361	C		
A	314	C		
A	305	C		
A	299	C		
A	297	C		
A	283	C		
A	209	C		
A	307	P		
A	282	P		
A	255	P		
A	254	P		
A	119	P		
B	375	C	302 a	22
B	369	C		
B	347	C		
B	334	C		
B	327	C		
B	310	C		
B	303	C		
B	307	P		
B	288	P		
C	383	C	321 a	30
C	350	C		
C	348	C		
C	342	C		
C	339	C		
C	329	C		
C	322	C		
C	300	C		
C	336	P		
C	323	P		
C	310	P		
C	309	P		
C	291	P		
C	265	P		
D	387	C	372 a	29
D	385	C		
D	383	C		
D	377	C		
D	376	C		
D	375	C		
D	379	P		
D	369	P		
D	364	P		
D	358	P		
D	356	P		
D	341	P		
E	354	C	314 a	38
E	337	C		
E	329	C		
E	326	C		
E	324	C		
E	322	C		
E	310	P		
E	310	P		
E	290	P		



## Appendix C

Program	Program	Program	Program	Program	Program
1. 1000	1. 1000	1. 1000	1. 1000	1. 1000	1. 1000
2. 1000	2. 1000	2. 1000	2. 1000	2. 1000	2. 1000
3. 1000	3. 1000	3. 1000	3. 1000	3. 1000	3. 1000
4. 1000	4. 1000	4. 1000	4. 1000	4. 1000	4. 1000
5. 1000	5. 1000	5. 1000	5. 1000	5. 1000	5. 1000
6. 1000	6. 1000	6. 1000	6. 1000	6. 1000	6. 1000
7. 1000	7. 1000	7. 1000	7. 1000	7. 1000	7. 1000
8. 1000	8. 1000	8. 1000	8. 1000	8. 1000	8. 1000
9. 1000	9. 1000	9. 1000	9. 1000	9. 1000	9. 1000
10. 1000	10. 1000	10. 1000	10. 1000	10. 1000	10. 1000

## Ceramography Protocols

### Sectioning

Equipment: Buehler Isomet 1000 Diamond Saw with 6" diamond blade (medium concentration)

Settings: Speed - 975 rpm, Load - 500 grams, and Lubricant – 2% solution of Allied cutting fluid

### Mounting

Equipment: Buehler 1.25" mounting cups, vacuum mounting chamber  
Settings: 5:3 ratio of Buehler low-viscosity epoxy to hardener, Vacuum applied for 10 minutes, and Mounts cured overnight

### Polishing

Equipment: Buehler Ecomet IV/Automet III Automated polishing system;  
with

five-sample holder.

Settings: See Table A.1

**Table C-1: Polishing Procedure for Silicon Carbide and Boron Carbide**

Surface	Time	Pressure (kgs/sample)	Speed (rpm)	Polishing Agent	Lubricant	Direction
Buehler 45 $\mu\text{m}$ Diamond Disc	Until Flat	3.628 kgs	150	none	Metadi + tap water	Clockwise
Buehler 15 $\mu\text{m}$ Diamond Disc	4 min	3.175 kgs	150	none	Metadi + tap water	Counterclockwise
Buehler Texmet	4 min	3.175 kgs	150	6 $\mu\text{m}$ Diamond	Metadi	Counterclockwise
Buehler Texmet	4 min	3.175 kgs	150	3 $\mu\text{m}$ Diamond	Metadi	Counterclockwise
Buehler Microcloth	4 min	3.175 kgs	150	Masterpolish 2	DI water	Clockwise



## **Chemical Etching (Silicon Carbide)**

Equipment: Hot plate, beakers tongs  
Settings: Murkami's reagent – 60g potassium ferricyanide, 60g potassium hydroxide, 120 ml H<sub>2</sub>O, Etchant brought to a boil; samples immersed 10-15 minutes

## **Electrolytic Etching (Boron Carbide)**

Equipment: Power Supply, plastic test cell, magnetic stirrer  
Settings: Electrolyte 1% KOH, 10V, 0.2 A/cm<sup>2</sup>, 30 seconds with agitation

---

## **X-Ray Diffraction Test Protocol**

### **Sample Preparation**

Samples sectioned to 1 cm<sup>2</sup> area and 1.5875 mm thick.  
Sample surfaces smoothed with 15 μm diamond disc  
Sample pieces affixed to circular Teflon XRD sample holders with double-sided tape

### **XRD Test Parameters**

Instrument: Siemens (Bruker) D5005  
Power: 45kV, 40 mA  
Count Time: 1 sec  
Step Size: 0.04° 2θ  
Scan Range: 30° to 75° 2θ

---

## **Flexure Testing Protocol**

### **Sample Preparation**

Samples sectioned to 4.064 x 3.048 x 45.72 mm in size  
Sample surfaces smoothed in two stages with 45 μm diamond disc, followed by 45 μm diamond disc

### **Flexure Test Parameters**

Instrument: Instron Model 1000  
Load Cell: 453.59 kgs  
Bearing Diameters: 9.525 mm

Load Diameter:	9.525 mm
Support Span:	38.1 mm
Crosshead Speed:	0.508 cm/min

---

## **Microindentation Measurement Protocol**

### **Sample Preparation**

Samples were prepared by polishing as described in Table A.1; samples were not relief polish or etched.

Samples Size: 0.5 cm<sup>2</sup>

### **Microindentation Parameters**

Load:	0 g
Dwell Time:	15 seconds
Number of Runs:	10

---

## **Density Measurements Protocol**

### **Sample Preparation**

Samples sectioned to fit in 1cc pycnometer cup  
Samples weighed to nearest 0.0001g

### **Helium Pycnometry Test Parameters**

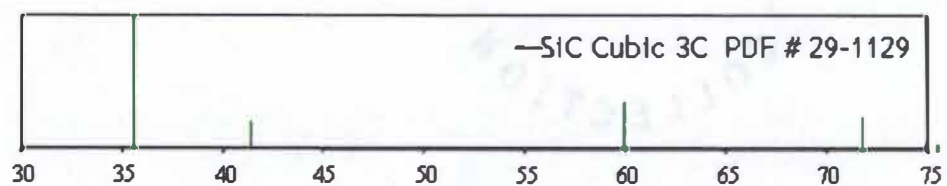
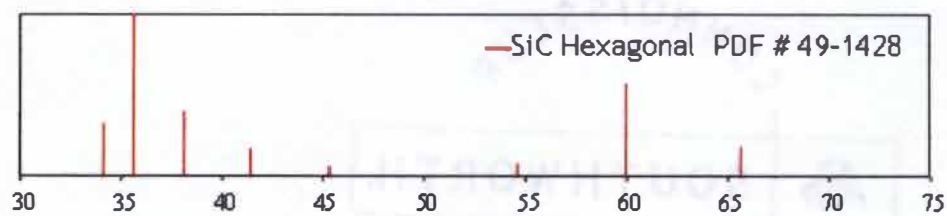
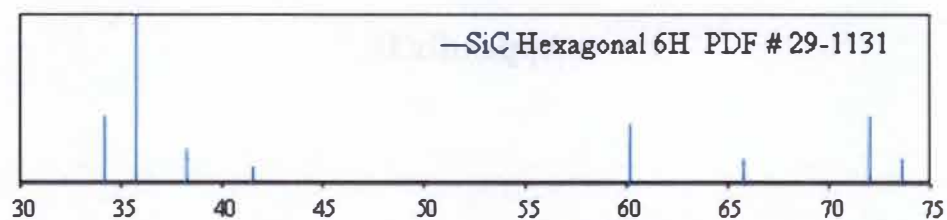
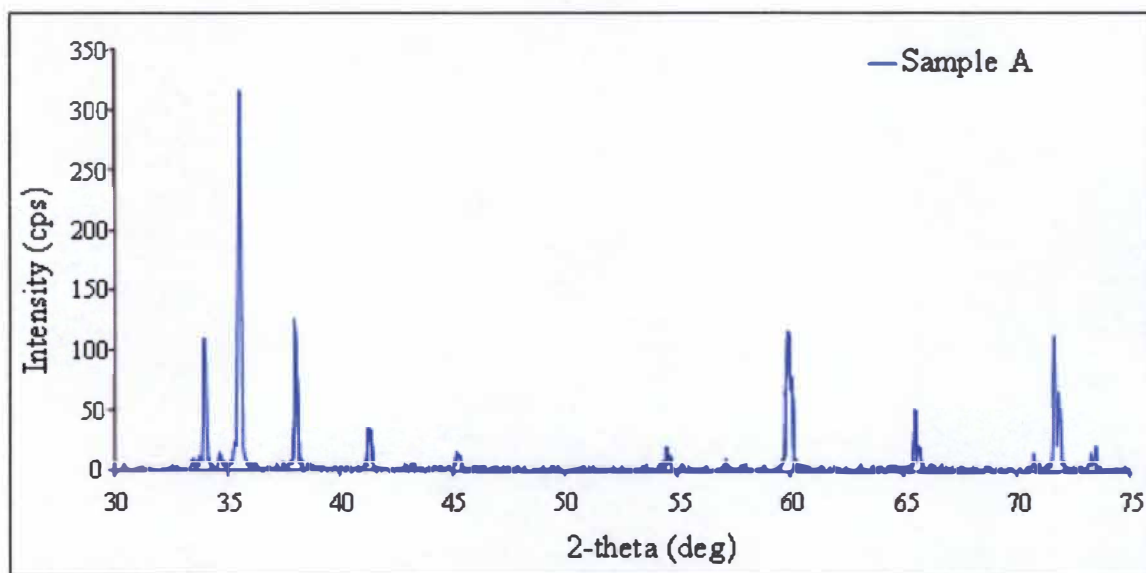
Instrument:	Micromeritics Accupyc 1330 (1cc) model
Gas:	Ultra high purity helium
Number of purges:	15
Number of runs:	20
Run Precision Criteria:	0.02%

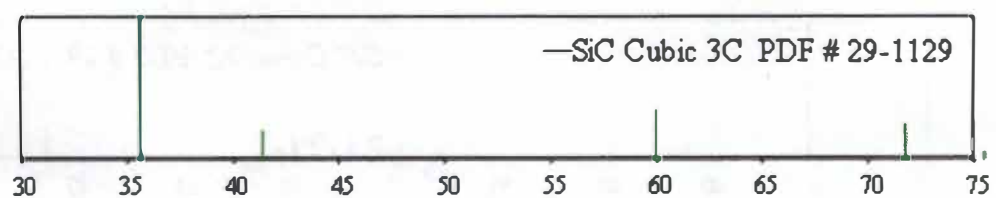
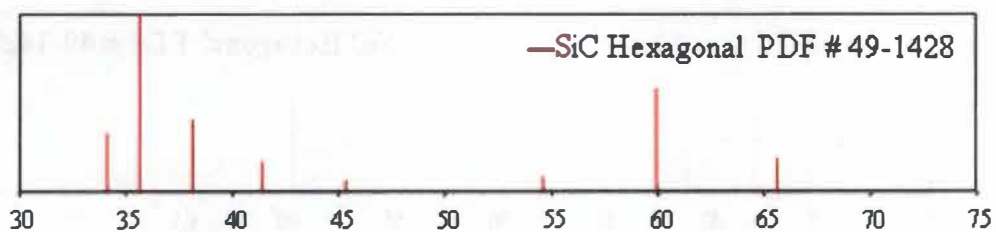
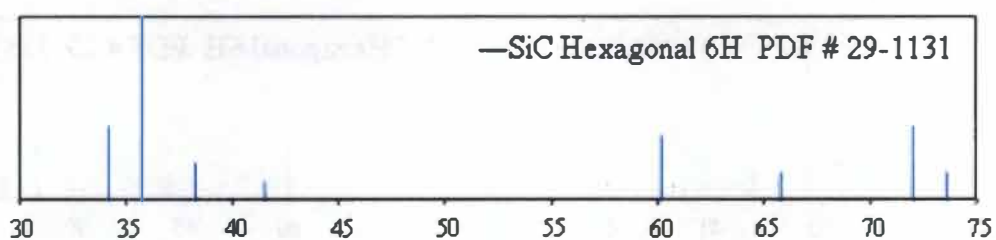
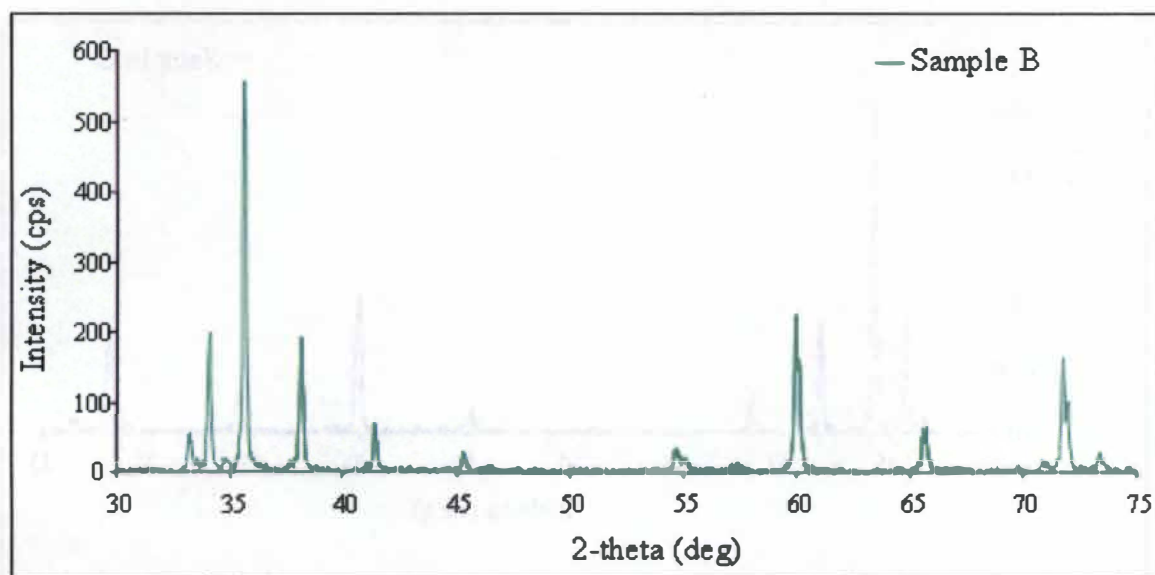


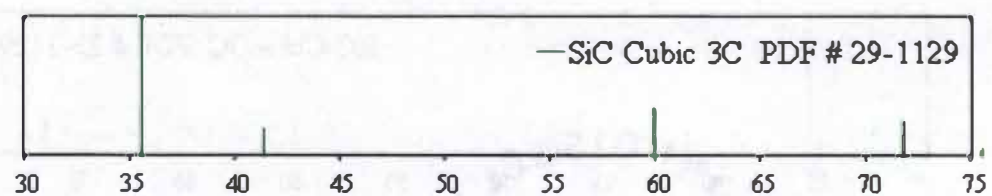
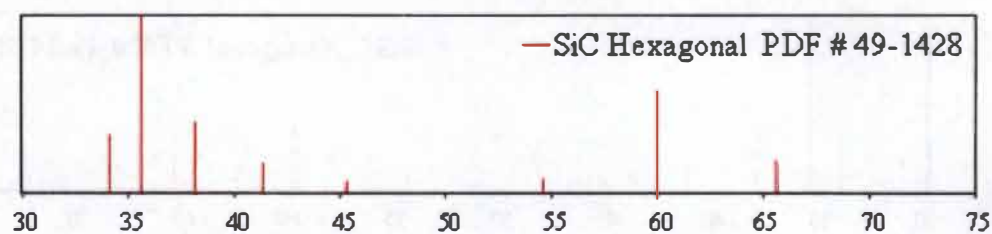
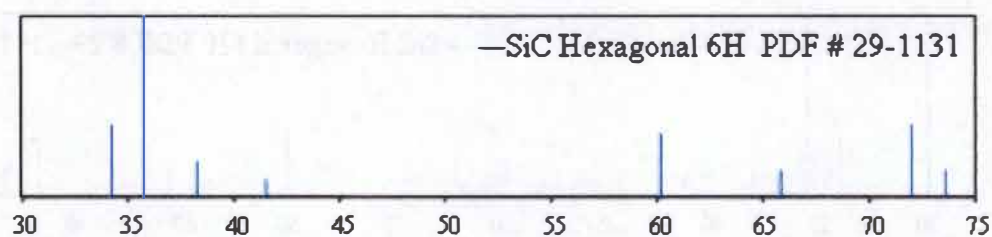
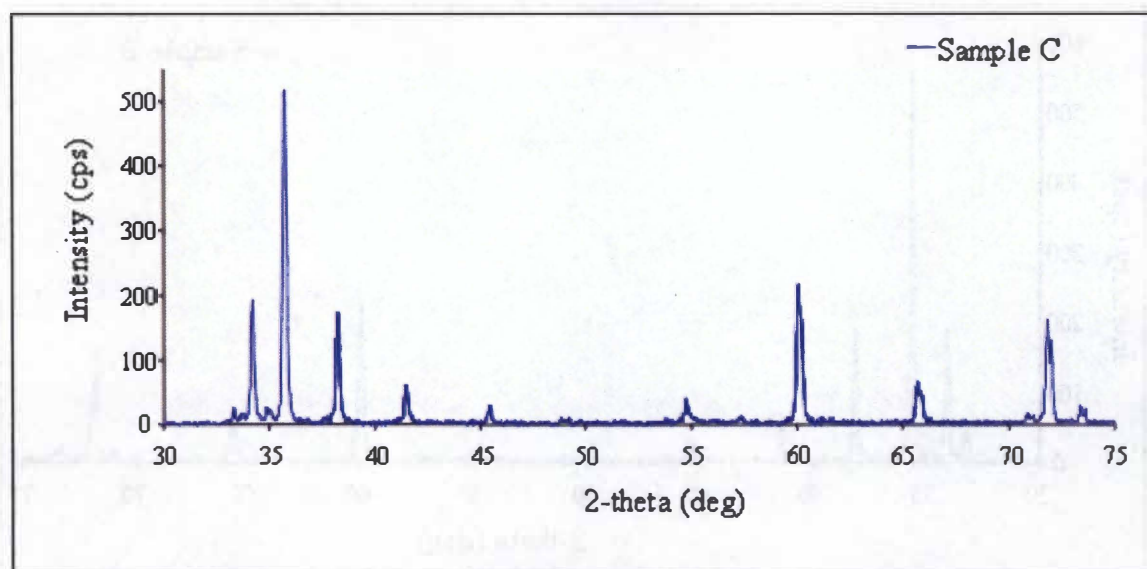
## Appendix D

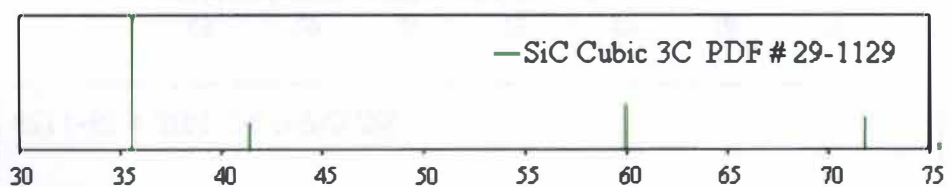
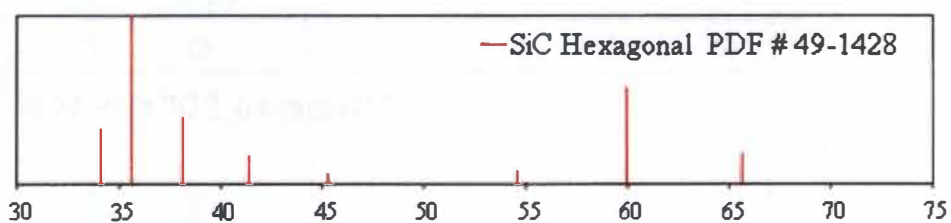
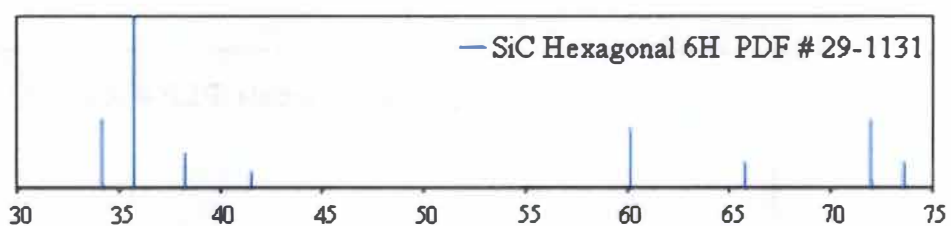
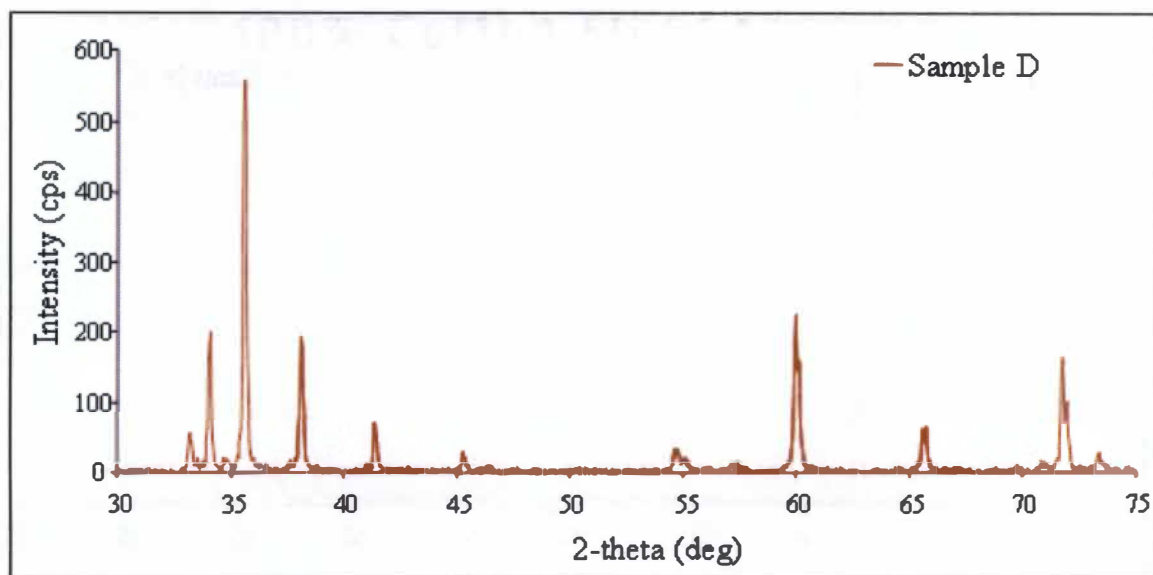


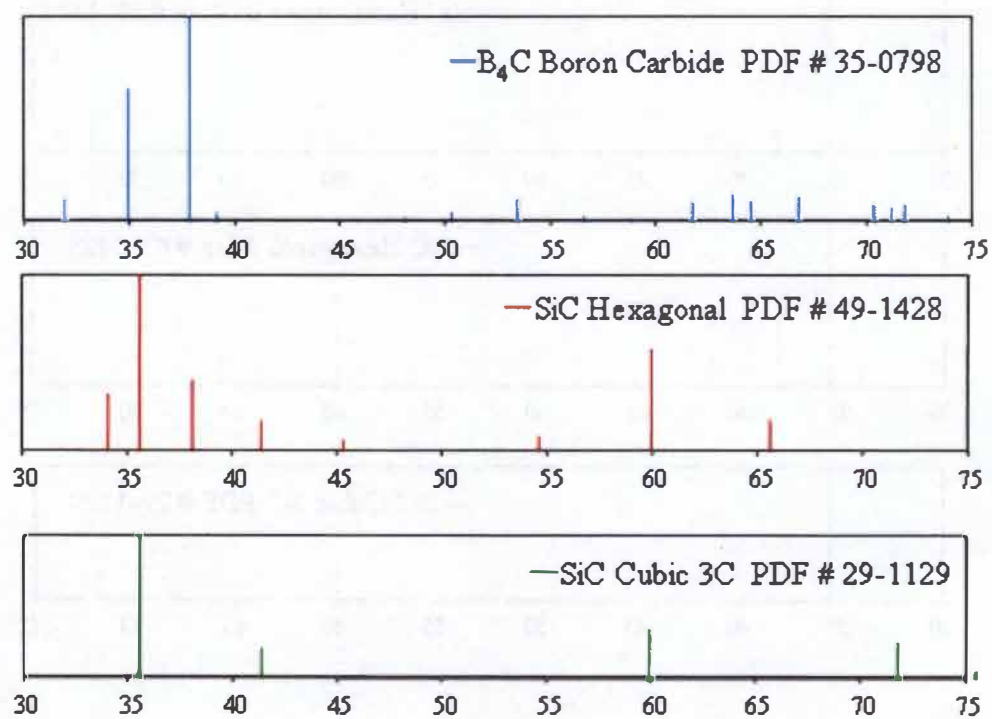
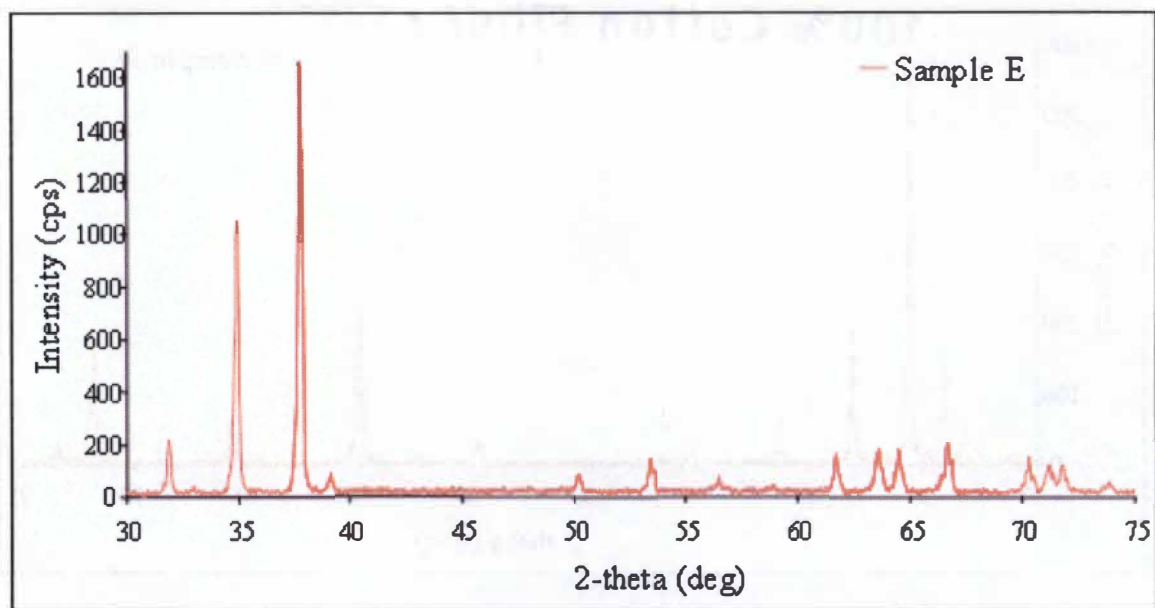
## X-Ray Diffraction (XRD) Plots













## **Vita**

Adolphus McDonald, Jr. was born in Syracuse, New York on October 8, 1960. He grew up on the south side of Syracuse, New York where he went to grade school at Percy Hughes, and high school at Roosevelt Junior High. He graduated from Christian Brothers Academy in 1978. From there, he went to Alabama A & M University, at Normal, Alabama, and received a Bachelor of Science degree in Mechanical Engineering Technology in 1982. From there he went to the University of Alabama, Huntsville, and received Bachelor of Science degree in Mechanical Engineering in 1992.

Adolphus will be receiving his Master of Science degree in Engineering Science at the University of Tennessee, Knoxville, December 2005.

